

Algorithmic construction of SSA-compatible extreme rays of the subadditivity cone and the $N = 6$ solution

Temple He,^a Veronika E. Hubeny,^b Massimiliano Rota^{b,c}

^aWalter Burke Institute for Theoretical Physics

California Institute of Technology, Pasadena, CA 91125 USA

^bCenter for Quantum Mathematics and Physics (QMAP)

Department of Physics & Astronomy, University of California, Davis, CA 95616 USA

^cSchool of Mathematics, University of Bristol, Woodland Road, Bristol, BS8 1UG UK

E-mail: templehe@caltech.edu, veronika@physics.ucdavis.edu,
max.rota@bristol.ac.uk

ABSTRACT: We compute the set of all extreme rays of the 6-party subadditivity cone that are compatible with strong subadditivity. In total, we identify 208 new (genuine 6-party) orbits, 52 of which violate at least one known holographic entropy inequality. For the remaining 156 orbits, which do not violate any such inequalities, we construct holographic graph models for 150 of them. For the final 6 orbits, it remains an open question whether they are holographic. Consistent with the strong form of the conjecture in [1], 148 of these graph models are trees. However, 2 of the graphs contain a “bulk cycle”, leaving open the question of whether equivalent models with tree topology exist, or if these extreme rays are counterexamples to the conjecture. The paper includes a detailed description of the algorithm used for the computation, which is presented in a general framework and can be applied to any situation involving a polyhedral cone defined by a set of linear inequalities and a partial order among them to find extreme rays corresponding to down-sets in this poset.

Contents

1	Introduction	1
2	Preliminaries	8
2.1	The mutual information poset and Klein’s condition	9
2.2	The Bell pairs theorem and additional constraints	10
3	The algorithm	13
3.1	Set-up	14
3.2	Closure operators	16
3.3	The algorithm in detail	19
3.4	A few possible variations	29
4	A simple example: $N = 5$	30
5	Results for $N = 6$	34
5.1	The approximation of SSA by KC is not exact	38
5.2	Extreme rays that violate holographic entropy inequalities	38
5.3	Extreme rays realizable by holographic graph models	40
5.4	Mystery extreme rays	42
6	Discussion	42

1 Introduction

The study of correlations is of central importance in quantum information theory, as it provides a comprehensive understanding of how information is distributed among different parts of a quantum system. Correlations are often explored through various entropy inequalities and related measures, which help in understanding the fundamental limits and capabilities of quantum systems, guiding the development of quantum technologies and deepening our theoretical understanding of quantum mechanics.

Motivated by research in quantum gravity, in particular in the context of gauge/gravity duality [2–4], a deep question about fundamental possible “patterns of dependences” in quantum mechanics was raised in [5], which dubbed it the *quantum marginal independence problem* (QMIP). In its simplest and most intuitive form, the QMIP asks the following question: Given the binary specification of presence versus absence of correlations between all pairs of disjoint subsystems, does there exist any quantum state realizing such a choice? As indicated in the following, the solution to this innocuously simple question is remarkably powerful. Below, we will specify certain aspects of this problem more fully, then motivate and contextualize them, and finally explain our strategy to tackle them.

Formulation of the problem: Let us label the parties $1, 2, \dots, N$, and denote the purifier 0 , and let $\underline{\mathcal{J}}, \underline{\mathcal{K}}$ denote an arbitrary pair of disjoint subsystems, i.e., $\underline{\mathcal{J}}, \underline{\mathcal{K}} \subseteq \llbracket N \rrbracket = \{0, 1, \dots, N\}$ with $\underline{\mathcal{J}} \cap \underline{\mathcal{K}} = \emptyset$. Suppose that for each such pair we only specify whether the two subsystems are correlated or not, without any further specification about the amount or other properties of such correlations. Under what conditions does there exist a *pure* quantum state such that all these demands are satisfied?

As explained in [5], and then further elaborated in [6], one can conveniently avoid unnecessary consideration of many obviously unrealizable patterns by reformulating the QMIP in terms of faces of the *subadditivity cone* (SAC). To define the SAC, one works in the space of subsystem von Neumann entropies. For an arbitrary N -party density matrix ρ_N , one first defines its *entropy vector* to be

$$\vec{S}(\rho_N) = \{S_{\underline{\mathcal{J}}}, \forall \underline{\mathcal{J}} \text{ such that } \emptyset \neq \underline{\mathcal{J}} \subseteq \llbracket N \rrbracket\}, \quad (1.1)$$

where components are ordered according some fixed convention (e.g., lexicographically), and $S_{\underline{\mathcal{J}}}$ is the von Neumann entropy of the reduced density matrix on the $\underline{\mathcal{J}}$ subsystem (notice the distinction between indices $\underline{\mathcal{J}} \subseteq \llbracket N \rrbracket$ and $\mathcal{J} \subseteq [N]$). The vector space \mathbb{R}^D with $D = 2^N - 1$, where this vector lives, will be called *N -party entropy space*.¹ The N -party subadditivity cone SAC_N is then defined as the *polyhedral* cone in N -party entropy space specified by all instances of *subadditivity* (SA), namely for any two disjoint nonempty subsystems $\underline{\mathcal{J}}, \underline{\mathcal{K}}$,

$$S_{\underline{\mathcal{J}}} + S_{\underline{\mathcal{K}}} \geq S_{\underline{\mathcal{J}\mathcal{K}}}, \quad (1.2)$$

where we used the conventional compact notation $S_{\underline{\mathcal{J}\mathcal{K}}}$ for $S_{\underline{\mathcal{J}} \cup \underline{\mathcal{K}}}$, and if $\underline{\mathcal{J}}$ contains the purifier 0 , we implicitly replace $S_{\underline{\mathcal{J}}}$ with the equivalent $S_{\underline{\mathcal{J}}^c}$ (and likewise for $\underline{\mathcal{K}}$ and $\underline{\mathcal{J}\mathcal{K}}$).²

Since (1.2) vanishes in quantum mechanics if and only if $\rho_{\underline{\mathcal{J}\mathcal{K}}} = \rho_{\underline{\mathcal{J}}} \otimes \rho_{\underline{\mathcal{K}}}$, which means there are no correlations between $\underline{\mathcal{J}}$ and $\underline{\mathcal{K}}$, the pattern of (in)dependences among the subsystems of an arbitrary purification of ρ_N (or equivalently, an arbitrary quantum state involving $N + 1$ parties) is completely captured by the unique *face* \mathcal{F} of the SAC_N for which

$$\vec{S}(\rho_N) \in \text{int}(\mathcal{F}), \quad (1.3)$$

with $\text{int}(\mathcal{F})$ denoting the interior of \mathcal{F} according to the standard topology of \mathbb{R}^D .³ The QMIP then asks for which faces of the SAC_N does there exist a density matrix ρ_N such that (1.3) holds. A face for which such a density matrix exists will be said to be *realizable*.⁴

Context and motivation: This formulation of the QMIP makes it obvious that the problem can easily be solved if one knows all the N -party entropy inequalities. Indeed, for

¹ We will call an arbitrary element of this vector space an entropy vector, even if it is not necessarily the vector of entropies of a density matrix as defined in (1.1).

² We also implicitly assume $S_{\emptyset} = 0$.

³ Since any face \mathcal{F} is specified by a set of SA instances which are saturated, if $\vec{S}(\rho_N) \in \partial\mathcal{F}$, then there is a lower-dimensional face $\mathcal{F}' \subset \mathcal{F}$ such that $\vec{S}(\rho_N) \in \text{int}(\mathcal{F}')$.

⁴ In some situations, it might be useful to slightly relax this definition of realizability and allow for the possibility that an entropy vector in the interior of a face is only approximated arbitrarily well by a density matrix (see e.g., [7]). This distinction however will not play a role here.

any given face \mathcal{F} of the SAC_N , one simply needs to check if there is at least one entropy vector in the interior of \mathcal{F} that satisfies all inequalities. A more interesting perspective instead is to interpret the QMIP as a more fundamental problem in quantum mechanics that could be solved by other means, and then ask what are the implications of its solution for the existence of new entropy inequalities, and what form they might have. If such solution is known up to some N , it is easy to see that the information it carries about N -party inequalities is very limited. This seems to change dramatically however, at least in some restricted scenarios, if one instead asks how much information about the N -party entropy inequalities is encoded in the solution to the QMIP for *all* $N' \geq N$ (or possibly for all $N' \leq f(N)$ for some function f).

In quantum gravity, there is strong evidence supporting the conjecture [1] that this knowledge is in fact sufficient to derive all entropy inequalities that characterize the *holographic entropy cone* [8]. Specifically, in this context one can define a restricted version of the QMIP, called the *holographic marginal independence problem* (HMIP), where instead of considering which faces can be realized by arbitrary quantum states, one focuses on the restricted class of “geometric states.”⁵ For any given number of parties N , it was argued in [1] that if one knows the solution to the HMIP *for each* $N' \geq N$, then one can in principle reconstruct all the inequalities that specify the N -party holographic entropy cone. In fact, [1] suggested that there might be an even more remarkable structure which only requires the solution to the “extremal” version of the HMIP rather than the full one. More precisely, let $\mathcal{R}_{\text{SA}}^N$ be the set of all 1-dimensional faces, or *extreme rays* (ERs), of the SAC_N , and $\mathcal{R}_{\text{Hoi}}^N \subseteq \mathcal{R}_{\text{SA}}^N$ be the subset of these that can be realized holographically.⁶ Then [1] argued that for any N , there exists some $N' \geq N$ (which depends on N) such that $\mathcal{R}_{\text{Hoi}}^{N'}$ provides sufficient information to derive the extreme rays of the N -party holographic entropy cone via a simple coarse-graining of subsystems. These then allow for a straightforward reconstruction of all the N -party holographic entropy inequalities (although in practice this might be a hard computation). The result of [1] is quite striking since the SAC itself is a much more primitive construct than the holographic entropy cone. It originates from the self-evident statement that the amount of correlation between any pair of subsystems cannot be negative, and as such it is not cognizant of holography. Indeed, the holographic input enters through the restriction to $\mathcal{R}_{\text{Hoi}}^N$.

Interestingly, even though [1] relied on technology only applicable in the holographic setting, a clue hinting at a similar structure in more general contexts was found recently in [7], which considered how to derive inner bounds to the general *quantum entropy cone* [11–14] from the solution to the QMIP. Denoting by $\mathcal{R}_{\text{Sta}}^N \subseteq \mathcal{R}_{\text{SA}}^N$ the set of extreme rays of the SAC_N that can be realized by *stabilizer states*, the main result of [7] was that a subset of $\mathcal{R}_{\text{Sta}}^9$ is sufficient to derive⁷ an inner bound to the 4-party quantum entropy cone which coincides with the full 4-party *stabilizer cone* [15].

⁵ These are the states of a holographic CFT that describe a classical bulk geometry, for which the entanglement entropy of a subsystem is computed by the HRRT prescription [9, 10].

⁶ Similarly, we will use \mathcal{R}^N with other subscripts to indicate subsets of the SAC_N extreme rays pertaining to the class indicated by the subscript; refer to Table 1 for a summary of these.

⁷ As in the holographic case, by derive we mean via subsystems coarse-grainings.

These results suggest that a similar structure might also exist at a more abstract level. For $N \geq 3$, most faces of the SAC_N cannot be part of the solution to the QMIP for the simple reason that they are “ruled out” by *strong subadditivity* (SSA). Following [6], we will say that a face is *SSA-compatible* if there is at least one entropy vector in its interior that satisfies all instances of SSA. For a fixed N , the set of SSA-compatible faces has the structure of a lattice,⁸ where the partial order is given by reverse inclusion ($\mathcal{F}_1 < \mathcal{F}_2$ if $\mathcal{F}_1 \supset \mathcal{F}_2$), and the meet of two faces is the lowest dimensional face $\mathcal{F} = \mathcal{F}_1 \wedge \mathcal{F}_2$ that includes \mathcal{F}_1 and \mathcal{F}_2 on its boundary [6].⁹ In general, the subset $\mathcal{R}_{\text{SSA}}^N \subseteq \mathcal{R}_{\text{SA}}^N$ of SSA-compatible extreme rays of the SAC_N is a subset of the set of coatoms of this lattice,¹⁰ but [6] showed that for $N \geq 4$ the lattice is not coatomistic. This means that not every element of the lattice can be obtained as the meet of a collection of coatoms. In other words, even geometrically, knowing $\mathcal{R}_{\text{SSA}}^N$ is in general insufficient information to be able to recover all the SSA-compatible higher-dimensional faces.¹¹ This result strongly suggests that in general, the solution to the QMIP for fixed N cannot be deduced from the solution $\mathcal{R}_{\text{QM}}^N$ of its extremal version for the same N , and that one needs to know all the meet-irreducible elements of the lattice.¹² For $N = 4$ however, it was already shown in [5] that all SSA-compatible faces of the SAC_4 are realizable in quantum mechanics, and that in fact stabilizer states are sufficient. This implies that the meet-irreducible elements of the lattice of SSA-compatible faces of the SAC_4 which are not coatoms can be obtained from coarse-grainings of certain coatoms of the analogous lattice for $N = 9$. In other words, similar to the holographic case, the solution to the QMIP can be derived from the solution to its extremal version involving a larger number of parties. All these observations suggest that there might be classes of quantum states for which the solution to the extremal marginal independence problem for all $N' \geq N$ carries a lot of (if not complete) information about the solution to the (seemingly) more general N -party QMIP, and even about entropy inequalities. This motivates us to study the set $\mathcal{R}_{\text{SSA}}^N$ more closely.

Another important motivation for us to study $\mathcal{R}_{\text{SSA}}^N$ comes again from holography. Suppose that the conjecture of [1] is true, and that all N -party holographic entropy inequalities can indeed be recovered from $\mathcal{R}_{\text{Hol}}^{N'}$ for some $N' \geq N$. Then what characterizes the extreme rays that can be realized in quantum mechanics but not by geometric states? A first guess, informed by data for $N \leq 5$, is that no such rays exist and $\mathcal{R}_{\text{QM}}^N = \mathcal{R}_{\text{Hol}}^N$. In other words, all extreme rays of the SAC_N that can be realized in quantum mechanics would also be

⁸ A lattice is a poset \mathcal{P} endowed with the additional property that for any two elements $x, y \in \mathcal{P}$, there exists both a least upper bound (called the join and denoted $x \vee y$) and a greatest lower bound (called the meet and denoted $x \wedge y$).

⁹ The set of faces of an arbitrary polyhedral cone forms a lattice with the same partial order and meet operation.

¹⁰ For $N \leq 4$, each coatom is an extreme ray, but it is not known if the inclusion is strict for larger N ; see [6] for more details.

¹¹ Technically, this result was proven for the set of SSA-compatible faces, which are not necessarily all realizable by quantum states. Therefore, it could have been in principle possible that each element of the lattice which is not the meet of a collection of coatoms is non-realizable, implying that the sublattice of realizable elements is coatomistic. However, we will see momentarily that already for $N = 4$ this is not true.

¹² An element x of a lattice is said to be meet-irreducible if $x = y \wedge z$ implies $x = y$ or $x = z$.

realizable holographically. This however was shown to be false in [16], which proved the strict inclusion $\mathcal{R}_{\text{Hol}}^N \subset \mathcal{R}_{\text{QM}}^N$ for $N \geq 6$ via the construction of an explicit counterexample, namely an extreme ray of the SAC_6 that can be realized by a stabilizer state but not by a geometric state.

To explore all these questions, it is useful to compute $\mathcal{R}_{\text{SSA}}^N$ for larger N , so that we have more data available for further investigations. In principle, the most straightforward way to derive $\mathcal{R}_{\text{SSA}}^N$ is to first find $\mathcal{R}_{\text{SA}}^N$, and then check which extreme rays satisfy SSA. This strategy however quickly runs into problems as N grows. For any given N , the number of facets of the SAC_N is given by

$$\text{number of facets} = \left\{ \begin{matrix} N+2 \\ 3 \end{matrix} \right\} - 2^N + 1, \quad (1.4)$$

where $\left\{ \begin{matrix} n \\ k \end{matrix} \right\}$ is the Stirling number of the second kind [17].¹³ For $N \leq 4$ the problem is easily manageable by freely available software [18], but the $N = 5$ case is already significantly more involved, since $D = 31$ and there are 270 facets. The computation can be largely simplified using a result of [6], which identified for arbitrary N a specific lower-dimensional face \mathcal{F}_* of the SAC_N that includes all elements of $\mathcal{R}_{\text{SSA}}^N$ (with the exception of the trivial ones corresponding to the Bell pairs).¹⁴ In general, the dimension of \mathcal{F}_* is given by

$$\dim(\mathcal{F}_*) = 2^N - \binom{N+1}{2} - 1, \quad (1.5)$$

which for $N = 5$ gives $\dim(\mathcal{F}_*) = 16$. Furthermore, upon dimensional reduction of the inequalities that specify the SAC_5 to the linear subspace spanned by \mathcal{F}_* , many inequalities become redundant and \mathcal{F}_* only has 80 facets. In this manner, the computation of $\mathcal{R}_{\text{SA}}^5$ becomes straightforward using [18], but as one can immediately see from (1.4) and (1.5), this simplification quickly becomes insufficient as N grows. Indeed, already at $N = 6$, the face \mathcal{F}_* has $\dim(\mathcal{F}_*) = 42$ and is specified by 280 inequalities (the number of facets of SAC_6 is 903), rendering the computation of $\mathcal{R}_{\text{SA}}^6$ unfeasible on a standard laptop. The set $\mathcal{R}_{\text{SA}}^7$ is certainly beyond reach, and the development of an algorithm that allows us to circumvent at least some of these difficulties will be the main goal of this paper.

Strategy: A simple observation, which is key to the development of this algorithm, is that already for small values of N the vast majority of extreme rays of the SAC_N violate SSA, i.e., $|\mathcal{R}_{\text{SSA}}^N| \ll |\mathcal{R}_{\text{SA}}^N|$.¹⁵ Since we are only interested in $\mathcal{R}_{\text{SSA}}^N$, one may then wonder whether there is a way to find this set more directly, without first deriving $\mathcal{R}_{\text{SA}}^N$. A possible strategy would be to first find all the extreme rays of the “SSA-cone”, the polyhedral cone in entropy space carved out by all instances of SA *and* SSA. It would then appear straightforward to extract the subset of extreme rays which are also elements of $\mathcal{R}_{\text{SA}}^N$. This strategy unfortunately suffers from the same issues described above, since the dimension

¹³ The number of SA instances is $\left\{ \begin{matrix} N+2 \\ 3 \end{matrix} \right\}$, but the $2^N - 1$ instances of the form $S_j \geq 0$ are not facets [6].

¹⁴ Since we will utilize this result in the computation presented in this paper, we will review it in detail in the next section.

¹⁵ This is evident already at $N = 3, 4$ (e.g., see [6]).

of the ambient space is the same, the number of facets is comparable, and most extreme rays of this cone are not elements of $\mathcal{R}_{\text{SSA}}^{\text{N}}$.

To focus on $\mathcal{R}_{\text{SSA}}^{\text{N}}$ without having to introduce new inequalities, we will instead consider a *variation* of what is perhaps the most basic (and in general inefficient) strategy to find the extreme rays of any polyhedral cone. Consider a vector space \mathbb{R}^n for some n , and a finite set \mathcal{E} of linear inequalities that specify a full-dimensional pointed¹⁶ cone \mathcal{C} . The set of vectors that saturate an inequality is a hyperplane in \mathbb{R}^n . An arbitrary subset $\mathcal{X} \subseteq \mathcal{E}$ then determines a linear subspace of \mathbb{R}^n given by the intersection of the hyperplanes in \mathcal{X} . If this subspace is 1-dimensional, one can then check if it contains a ray that satisfies all the inequalities in \mathcal{E} . If such a ray exists, it is obviously an extreme ray of \mathcal{C} . By considering all possible subsets $\mathcal{X} \in 2^{\mathcal{E}}$, we can in principle find all the extreme rays. We call this strategy the “brute force strategy.”

The inefficiency of this procedure should be obvious, but what if one is only interested in a subset of extreme rays and can drastically reduce the search space from $2^{\mathcal{E}}$ to a much smaller subset? The essence of our method will be to apply the brute force strategy to a sufficiently reduced search space. As we will review in detail, such a reduction can be attained using the strategy of [6], where one replaces SSA with a weaker condition, dubbed *Klein’s condition* (KC), that can be conveniently phrased in terms of collections of SA instances. Following [6], we will formulate KC by introducing a partial order among the SA instances. The set $\mathcal{R}_{\text{KC}}^{\text{N}}$ of extreme rays of the SAC_{N} that obey this condition will be the set of extreme rays for which the corresponding sets of saturated SA instances are *down-sets*. The algorithm will take advantage of this structural property of extreme rays to restrict the search space from $2^{\mathcal{E}}$ to the lattice of down-sets of the poset. This is still far from being a sufficient reduction for $\text{N} \geq 6$, but using *closure operators* we will then “combine” this constraint with the dependences among the SA instances to reduce the search space even further.

Our algorithm will compute $\mathcal{R}_{\text{KC}}^{\text{N}}$, and since KC is an approximation to SSA, we have

$$\mathcal{R}_{\text{SSA}}^{\text{N}} \subseteq \mathcal{R}_{\text{KC}}^{\text{N}} \subseteq \mathcal{R}_{\text{SA}}^{\text{N}}. \quad (1.6)$$

To find $\mathcal{R}_{\text{SSA}}^{\text{N}}$, it then suffices to check which elements of $\mathcal{R}_{\text{KC}}^{\text{N}}$ satisfy SSA, which is a straightforward computation. The advantage of this strategy ultimately lies in the expectation that as N grows,

$$\frac{|\mathcal{R}_{\text{KC}}^{\text{N}}|}{|\mathcal{R}_{\text{SSA}}^{\text{N}}|} \ll \frac{|\mathcal{R}_{\text{SA}}^{\text{N}}|}{|\mathcal{R}_{\text{KC}}^{\text{N}}|}. \quad (1.7)$$

As verified in [6], for $\text{N} \leq 5$ we have $\mathcal{R}_{\text{KC}}^{\text{N}} = \mathcal{R}_{\text{SSA}}^{\text{N}}$ (in contrast to higher-dimensional faces of the SAC_{N}), which means at least for extreme rays the approximation of SSA by KC is exact. This led [6] to speculate that this equivalence might hold for arbitrary N . However, this is not true, and we will construct the simplest counterexamples for $\text{N} = 6$.

Preview of results: The set $\mathcal{R}_{\text{SSA}}^6$ is much richer than its counterparts for lower parties, and we can use our results in this paper to investigate various conjectures and questions

¹⁶ A cone is pointed if it does not contain any linear subspace other than the trivial subspace.

\mathcal{R}_{SA}	All the extreme rays (ERs) of the SAC
\mathcal{R}_{KC}	ERs of the SAC that satisfy KC
\mathcal{R}_{SSA}	ERs of the SAC that satisfy SSA
\mathcal{R}_{QM}	ERs of the SAC realizable by arbitrary quantum states
\mathcal{R}_{Sta}	ERs of the SAC realizable by stabilizer states
\mathcal{R}_{HyG}	ERs of the SAC realizable by hypergraph models
\mathcal{R}_{Hol}	ERs of the SAC realizable by graph models
\mathcal{R}_{TG}	ERs of the SAC realizable by tree graph models
\mathcal{R}_{STG}	ERs of the SAC realizable by simple tree graph models
\mathcal{R}_{\star}	ERs of the SAC realizable by star graph models

Table 1: Summary of the definitions of various classes of extreme rays of the SAC for a fixed value of N (to keep the table cleaner, we dropped the explicit dependence on N of each set).

$\mathcal{R}_{\star} \subseteq \mathcal{R}_{\text{STG}}$	Any star graph model is a simple tree graph model	[1, 8]
$\mathcal{R}_{\text{STG}} \subseteq \mathcal{R}_{\text{TG}}$	Any simple tree graph model is a tree graph model	[1, 8]
$\mathcal{R}_{\text{TG}} \subseteq \mathcal{R}_{\text{Hol}}$	Any tree graph model is a graph model	[1, 8]
$\mathcal{R}_{\text{Hol}} \subseteq \mathcal{R}_{\text{HyG}}$	Any graph model is a hypergraph model	[19]
$\mathcal{R}_{\text{HyG}} \subseteq \mathcal{R}_{\text{Sta}}$	Any hypergraph model can be realized by a stabilizer state	[20]
$\mathcal{R}_{\text{Sta}} \subseteq \mathcal{R}_{\text{QM}}$	Any stabilizer state is a quantum state	[15]
$\mathcal{R}_{\text{QM}} \subseteq \mathcal{R}_{\text{SSA}}$	Any quantum state satisfies SSA	[11, 21]
$\mathcal{R}_{\text{SSA}} \subseteq \mathcal{R}_{\text{KC}}$	KC is implied by SSA	[6, 22]
$\mathcal{R}_{\text{KC}} \subseteq \mathcal{R}_{\text{SA}}$	KC is a condition on the set of SA instances saturated by an ER	[6, 22]

Table 2: Inclusion relations for the various classes of extreme rays of the SAC. For each inclusion, we added references to the papers where it was proven, or where the structure in entropy space which defines the class was first introduced (when the inclusion follows automatically from the definition of the class).

that have appeared in previous work. In Table 1 we review the definition of various useful subsets of \mathcal{R}_{SA} , depending on whether they are realizable or, if they are, the class of quantum states that realizes them. These subsets satisfy the following chain of inclusions (see Table 2 for more details):

$$\mathcal{R}_{\star} \subseteq \mathcal{R}_{\text{STG}} \subseteq \mathcal{R}_{\text{TG}} \subseteq \mathcal{R}_{\text{Hol}} \subseteq \mathcal{R}_{\text{HyG}} \subseteq \mathcal{R}_{\text{Sta}} \subseteq \mathcal{R}_{\text{QM}} \subseteq \mathcal{R}_{\text{SSA}} \subseteq \mathcal{R}_{\text{KC}} \subseteq \mathcal{R}_{\text{SA}}. \quad (1.8)$$

For $N \leq 5$, Table 3 summarizes which inclusions are strict and which inclusions are in fact equalities. For $N \geq 6$, the current knowledge can instead be summarized as follows:

$$\mathcal{R}_{\star} \subset \mathcal{R}_{\text{STG}} \subset \mathcal{R}_{\text{TG}} \subseteq \mathcal{R}_{\text{Hol}} \subset \mathcal{R}_{\text{HyG}} \subseteq \mathcal{R}_{\text{Sta}} \subseteq \mathcal{R}_{\text{QM}} \subseteq \mathcal{R}_{\text{SSA}} \subset \mathcal{R}_{\text{KC}} \subset \mathcal{R}_{\text{SA}}, \quad (1.9)$$

where $\mathcal{R}_{\text{Hol}} \subset \mathcal{R}_{\text{HyG}}$ was shown in [16], and $\mathcal{R}_{\text{SSA}} \subset \mathcal{R}_{\text{KC}}$ will be shown in this paper.

Furthermore, a conjecture first proposed in [1] implies that $\mathcal{R}_{\text{TG}} = \mathcal{R}_{\text{Hol}}$, which we are able to explore in the $N = 6$ case in this paper. As we will see in more detail, the elements of $\mathcal{R}_{\text{SSA}}^6$ can be organized into 208 orbits under the symmetries of the problem, and out of these, 52 violate at least one known *holographic entropy inequality* (HEI) and are therefore not in $\mathcal{R}_{\text{Hol}}^6$. Of the remaining 156 orbits, we managed to construct an explicit graph model for 150 orbits, thereby proving that they are in $\mathcal{R}_{\text{Hol}}^6$. While 148 of these graph models

$N = 2$	$\mathcal{R}_* = \mathcal{R}_{\text{SA}}$	[1, 8]
$N = 3$	$\mathcal{R}_* = \mathcal{R}_{\text{KC}} \subset \mathcal{R}_{\text{SA}}$	[1, 8]
$N = 4$	$\mathcal{R}_* = \mathcal{R}_{\text{KC}} \subset \mathcal{R}_{\text{SA}}$	[1, 8]
$N = 5$	$\mathcal{R}_* \subset \mathcal{R}_{\text{STG}} = \mathcal{R}_{\text{KC}} \subset \mathcal{R}_{\text{SA}}$	[1, 23]
$N = 6$	See (1.9) and related references	

Table 3: Summary of the essential equivalencies and strict inclusions among the various classes for different values of N . Further equivalences follow automatically from the inclusions in Table 2.

indeed have a tree topology, two of them do not, therefore just falling short of verifying the conjecture $\mathcal{R}_{\text{TG}} = \mathcal{R}_{\text{Hol}}$ for $N = 6$. Of course, this result does not disprove the conjecture either, since we did not prove that there cannot be tree graph models realizing those two entropy vectors. Moreover, to get a definitive answer at $N = 6$, one would also need to determine whether the remaining six “mystery” orbits are holographic or not, and if so, whether they can be realized by trees.

Finally, we stress that our algorithm relies only on the existence of a partial order among the inequalities. This means it is not in any way specific to entropy inequalities such as SA. In fact, it can be used in any context where one is interested in finding not all extreme rays, but rather only the subset of extreme rays which correspond to down-sets in the poset.

The structure of the paper is as follows. In §2, we review the necessary definitions about the mutual information poset, how it can be used to formulate KC, and a few additional results from our previous work that we will use to simplify the computation of $\mathcal{R}_{\text{SSA}}^6$. The algorithm that we use is then presented in §3. We stress that this section is written independently from the set-up of the SAC reviewed in §2, and thus our algorithm can be immediately utilized for other applications. To exemplify how the algorithm works, we then re-compute the set $\mathcal{R}_{\text{SSA}}^5$ in §4. The result of the computation for $N = 6$ is presented in §5, along with a preliminary analysis of this data and all the holographic graph models that we were able to construct. Readers who are only interested in the results of the $N = 6$ case, and not in the details of the algorithm, can skip earlier sections and proceed directly to §5.¹⁷ Finally, in §6 we comment on open questions and future directions of investigation.

2 Preliminaries

An instance of SA (see (1.2)) can be written as

$$I(\underline{\mathcal{J}} : \underline{\mathcal{K}}) \equiv S_{\underline{\mathcal{J}}} + S_{\underline{\mathcal{K}}} - S_{\underline{\mathcal{J}\mathcal{K}}} \geq 0, \quad (2.1)$$

where $I(\underline{\mathcal{J}} : \underline{\mathcal{K}})$ is the *mutual information* (MI) between subsystems $\underline{\mathcal{J}}$ and $\underline{\mathcal{K}}$. Clearly, an instance of SA is saturated if and only if the corresponding MI instance vanishes. For any given N , we denote by \mathcal{E} the set of all MI instances.

We will review in this section the definition of Klein’s condition for a subset $\mathcal{X} \subseteq \mathcal{E}$, and how this can be formulated in terms of a poset. This will make manifest that in the

¹⁷ Further details regarding the various attributes of $\mathcal{R}_{\text{SSA}}^6$ are also presented in [24].

search for $\mathcal{R}_{\text{KC}}^{\text{N}}$ we can restrict the search space from the power-set $2^{\mathcal{E}}$ to the set of down-sets $\mathcal{X} \subseteq \mathcal{E}$ which include all minimal elements of the poset without containing any maximal, or even next-to-maximal, elements. The presentation will follow [6] closely, and we refer the reader to that paper for more details.

2.1 The mutual information poset and Klein's condition

Given a face \mathcal{F} of the SAC_{N} , consider an entropy vector $\vec{S} \in \text{int}(\mathcal{F})$ and the set of all MI instances that vanish for \vec{S} , i.e.,

$$\mathcal{V}(\vec{S}) = \{\underline{I}(\underline{J} : \underline{\mathcal{K}}) \in \mathcal{E}, \quad \underline{I}(\underline{J} : \underline{\mathcal{K}})(\vec{S}) = 0\}. \quad (2.2)$$

Notice that this set does not depend on the specific choice of \vec{S} in the interior of \mathcal{F} , and therefore we can naturally associate a set $\mathcal{V}(\mathcal{F})$ to a face \mathcal{F} . Furthermore, we stress that here \mathcal{F} and \vec{S} are not assumed to be realizable, and we can extend the map (2.2) to the full entropy space.

Since in quantum mechanics an MI instance vanishes if and only if the density matrix factorizes, we have the chain of implications

$$\underline{I}(\underline{J} : \underline{J}\underline{\mathcal{K}}) = 0 \implies \rho_{\underline{J}\underline{J}\underline{\mathcal{K}}} = \rho_{\underline{J}} \otimes \rho_{\underline{J}\underline{\mathcal{K}}} \implies \rho_{\underline{J}\underline{\mathcal{K}}} = \rho_{\underline{J}} \otimes \rho_{\underline{\mathcal{K}}} \implies \underline{I}(\underline{J} : \underline{\mathcal{K}}) = 0. \quad (2.3)$$

Motivated by this simple observation, we then define the following necessary condition for the realizability of a face of the SAC_{N} .

Definition 1 (Klein's condition (KC)). *A face \mathcal{F} of the SAC_{N} satisfies Klein's condition if for any three disjoint subsets $\underline{J}, \underline{J}$, and $\underline{\mathcal{K}}$,*

$$\underline{I}(\underline{J} : \underline{J}\underline{\mathcal{K}}) \in \mathcal{V}(\mathcal{F}) \implies \underline{I}(\underline{J} : \underline{\mathcal{K}}) \in \mathcal{V}(\mathcal{F}). \quad (2.4)$$

If a face \mathcal{F} satisfies KC we call it a KC-face, and in the 1-dimensional case, a KC extreme ray (KC-ER).

Notice that, given SA, this condition immediately follows from SSA, which can be written as

$$\underline{I}(\underline{J} : \underline{J}\underline{\mathcal{K}}) \geq \underline{I}(\underline{J} : \underline{\mathcal{K}}). \quad (2.5)$$

We can then interpret KC as an approximation of SSA, in the sense that any SSA-compatible face of the SAC_{N} is necessarily a KC-face. As anticipated in the Introduction, the advantage of this approximation is that it characterizes a subset of faces of the SAC_{N} that *could* be SSA-compatible purely in terms of SA.

Having defined KC, we now review how it can be conveniently rephrased in terms of a partially ordered structure. Recall that a poset $\mathcal{P} = (X, \preceq)$ is defined as a set X with a binary relation \preceq that is reflexive, antisymmetric, and transitive.¹⁸ We define the *mutual information poset* (MI-poset) as follows.

¹⁸That is, for all $x, y, z \in X$ we have (i) $x \preceq x$; (ii) if $x \preceq y$ and $y \preceq x$, then $x = y$; and finally (iii) if $x \preceq y$ and $y \preceq z$, then $x \preceq z$.

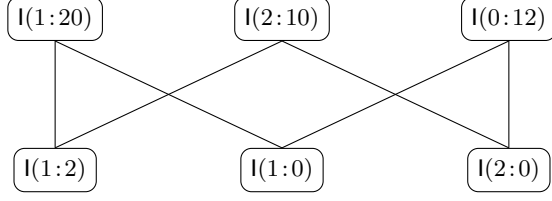


Figure 1: The Hasse diagram of the MI-poset for $N = 2$.

Definition 2 (Mutual information poset (MI-poset)). *For any given N , the mutual information poset (\mathcal{E}, \preceq) is the set of all MI instances \mathcal{E} with partial order given by the relation*

$$I(\mathcal{J} : \mathcal{K}) \preceq I(\mathcal{J}' : \mathcal{K}') \iff \mathcal{J} \subseteq \mathcal{J}' \text{ and } \mathcal{K} \subseteq \mathcal{K}' \text{ or } \mathcal{J} \subseteq \mathcal{K}' \text{ and } \mathcal{K} \subseteq \mathcal{J}'. \quad (2.6)$$

As a simple example, we have depicted the MI-poset for $N = 2$ in Figure 1 using a Hasse diagram. The lines denote covering relations, where an element x is joined to an element y if $x \prec y$, and there does not exist z such that $x \prec z \prec y$.

Given a poset \mathcal{P} , a *down-set* is defined as a subset of $Y \subseteq X$ such that for any $y \in Y$,

$$z \preceq y \implies z \in Y. \quad (2.7)$$

It then follows from the definition of the partial order in the MI-poset (2.6) and the definition of KC given in (2.4) that a face \mathcal{F} of the SAC_N is a KC-face only if $\mathcal{V}(\mathcal{F})$ is a down-set. It is important to notice that given an arbitrary down-set \mathcal{D} of the MI-poset, it is *not* necessarily the case that there exists a face \mathcal{F} such that $\mathcal{V}(\mathcal{F}) = \mathcal{D}$. An analogous statement also holds for arbitrary subsets $\mathcal{X} \subseteq \mathcal{E}$, and the underlying reason is in fact the same: Such arbitrary \mathcal{D} and \mathcal{X} do not necessarily respect the dependences among SA instances. For now, however, it is sufficient to notice that by focusing on down-sets of the MI-poset, we can restrict the search space for the brute force computation of $\mathcal{R}_{\text{SSA}}^N$ from the power-set $2^{\mathcal{E}}$ to the lattice of down-sets¹⁹ of the MI-poset, which is already significantly smaller. For example, for $N = 3$ we have $|2^{\mathcal{E}}| = 2^{25} = 33,554,432$, while the down-set lattice has cardinality 11,422.

2.2 The Bell pairs theorem and additional constraints

Having explained how to reduce the search space for $\mathcal{R}_{\text{SSA}}^N$ to down-sets of the MI-poset, we now review two constraints that can be used to ignore certain families of down-sets. The first result was already anticipated in the Introduction and allows us to focus on a specific face \mathcal{F}_* of the SAC_N which includes all KC-ERs that are not realized by Bell pairs. Since this face is realizable in quantum mechanics, it is a KC-face, and the set $\mathcal{V}(\mathcal{F}_*)$ must be a down-set. In particular, $\mathcal{V}(\mathcal{F}_*)$ is the set of minimal elements of the MI-poset [6].

Theorem 1 (Bell pairs theorem). *For any given number of parties N , any KC-compatible extreme ray of the SAC_N which is not realized by a single Bell pair obeys the condition*

$$I(\ell : \ell') = 0 \text{ for all } \ell, \ell' \in \llbracket N \rrbracket. \quad (2.8)$$

¹⁹The set of all down-sets of any poset, with partial order given by inclusion, has the structure of a lattice, where meet and join correspond respectively to intersection and union [25].

Proof. See Corollary 1 in [6]. □

This theorem implies that to find extreme rays which do not correspond to Bell pairs, we should only consider down-sets of the MI-poset which include all minimal elements, i.e., the MI instances between single parties. However, notice that since \mathcal{F}_* contains *all* KC-ERs except for those realized by Bell pairs, in particular it also contains trivial lifts of KC-ERs for any N' such that $3 \leq N' \leq N$ [6].

Suppose now that we want to compute $\mathcal{R}_{\text{SSA}}^N$ for some N , and that the sets $\mathcal{R}_{\text{SSA}}^{N'}$ for all $N' \leq N$ are already known. The second result that we review will allow us to only consider down-sets which are guaranteed to correspond to “genuine N -party” KC-ERs, therefore avoiding the reconstruction of extreme rays that we already know. Notice that the maximal elements of the MI-poset take the form

$$I(\underline{\mathcal{J}} : \underline{\mathcal{J}}^c) = S_{\underline{\mathcal{J}}} + S_{\underline{\mathcal{J}}^c} - S_{\llbracket N \rrbracket} = 2S_{\underline{\mathcal{J}}}, \quad (2.9)$$

where $\underline{\mathcal{J}}^c \equiv \llbracket N \rrbracket \setminus \underline{\mathcal{J}}$, and we utilized the assumption that the system on all $\llbracket N \rrbracket$ parties is pure.²⁰ Consider now a face \mathcal{F} of the SAC_N such that $\mathcal{V}(\mathcal{F})$ includes one such element. Assuming for simplicity that $\underline{\mathcal{J}}$ does not include the purifier $\ell = 0$ (if it does we can simply repeat the same argument for $\underline{\mathcal{J}}^c$), we can then denote $\underline{\mathcal{J}}$ by just \mathcal{J} and have $S_{\mathcal{J}} = 0$ for any vector $\vec{S} \in \mathcal{F}$. If \vec{S} is realizable by some density matrix ρ_N , then we can write it as

$$\rho_N = |\psi\rangle_{\mathcal{J}} \langle \psi|_{\mathcal{J}} \otimes \rho_{\mathcal{J}^c}, \quad (2.10)$$

where $|\psi\rangle_{\mathcal{J}}$ is a pure state and $\mathcal{J}^c \equiv \llbracket N \rrbracket \setminus \mathcal{J}$ (by itself purified by the purifier 0). The density matrix ρ_N is then a state of a system composed of two uncorrelated subsystems on $|\mathcal{J}|$ and $|\mathcal{J}^c|$ parties respectively. We can rewrite the entropy vector of this density matrix to be

$$\vec{S}(\rho_N) = \vec{S}(|\psi\rangle_{\mathcal{J}} \langle \psi|_{\mathcal{J}} \otimes \rho_{\mathcal{J}^c}) = \vec{S}(|\psi\rangle_{\mathcal{J}} \langle \psi|_{\mathcal{J}} \otimes |0\rangle_{\mathcal{J}^c} \langle 0|_{\mathcal{J}^c}) + \vec{S}(|0\rangle_{\mathcal{J}} \langle 0|_{\mathcal{J}} \otimes \rho_{\mathcal{J}^c}), \quad (2.11)$$

where $|0\rangle_{\mathcal{J}} \langle 0|_{\mathcal{J}}$ is a “completely decorrelated” state for subsystem \mathcal{J} .²¹ If \mathcal{F} is an extreme ray, any entropy vector $\vec{S}(\rho_N)$ generating it cannot be the sum of two distinct nontrivial vectors within the SAC. Therefore, the only possibility is that the first term is the null vector, which implies

$$|\psi\rangle_{\mathcal{J}} = |0\rangle_{\mathcal{J}} \implies \rho_N = |0\rangle_{\mathcal{J}} \langle 0|_{\mathcal{J}} \otimes \rho_{\mathcal{J}^c}. \quad (2.12)$$

Thus, the extreme ray associated to ρ_N is a “canonical” lift (see [6]) to N parties of the extreme ray associated to $\rho_{\mathcal{J}^c}$ of the SAC for $|\mathcal{J}^c|$ parties.

Indeed, we can use a similar argument to see that we can even ignore any down-set involving next-to-maximal elements in the MI-poset. Suppose our down-set includes an element of the form

$$I(\mathcal{J} : \mathcal{J}^c) = S_{\mathcal{J}} + S_{\mathcal{J}^c} - S_{\llbracket N \rrbracket}, \quad (2.13)$$

²⁰ This implies that $S_{\llbracket N \rrbracket} = S_{\emptyset} = 0$ and $S_{\mathcal{J}^c} = S_{\mathcal{J}}$.

²¹ In other words, $|0\rangle_{\mathcal{J}}$ is a tensor product of states for the individual parties in \mathcal{J} .

and we have assumed without loss of generality that the party not appearing in the arguments is the purifier. As in our argument above, assuming $\vec{S}(\rho_{\mathbf{N}})$ is realizable by some quantum state $\rho_{\mathbf{N}}$, this means we can write

$$\rho_{\mathbf{N}} = \rho_{\mathcal{J}} \otimes \rho_{\mathcal{J}^c}. \quad (2.14)$$

The entropy vector associated to this density matrix can be rewritten as

$$\vec{S}(\rho_{\mathbf{N}}) = \vec{S}(\rho_{\mathcal{J}} \otimes \rho_{\mathcal{J}^c}) = \vec{S}(\rho_{\mathcal{J}} \otimes |0\rangle\langle 0|_{\mathcal{J}^c}) + \vec{S}(|0\rangle\langle 0|_{\mathcal{J}} \otimes \rho_{\mathcal{J}^c}). \quad (2.15)$$

This implies that $\vec{S}(\rho_{\mathbf{N}})$ is the sum of two nontrivial entropy vectors in the \mathbf{N} -party entropy space, and hence $\vec{S}(\rho_{\mathbf{N}})$ cannot be an extreme ray. Notice that we cannot use this argument to further exclude MI-poset elements $\mathsf{l}(\mathcal{J} : \mathcal{K})$ below the next-to-maximal ones, since even if we still have a factorization of the density matrix as in (2.14), it would not involve all the \mathbf{N} parties. Finally, notice that for these arguments, we used the assumption that the face \mathcal{F} is realizable. The result however can be extended to any KC-face, independently from realizability, and we refer to reader to Section 3.4 of [6] for the proof and a more detailed discussion.

As an explicit example of these two results consider again the case of $\mathbf{N} = 3$. The number of down-sets that include all minimal elements is 8,695, and if we further demand that the down-sets do not include any maximal elements we are left with $2^{12} = 4,096$ possibilities. These correspond to all possible subsets of the antichain

$$\mathcal{A} = \{\mathsf{l}(\ell : \ell' \ell''), \text{ for all distinct } \ell, \ell', \ell'' \in \llbracket 3 \rrbracket\}. \quad (2.16)$$

However, consider for example a down-set \mathcal{D} composed of all minimal elements and $\mathsf{l}(1 : 23)$. Notice that

$$\mathsf{l}(1 : 23) + \mathsf{l}(1 : 0) = \mathsf{l}(1 : 230) = 2\mathsf{S}_1. \quad (2.17)$$

Since $\mathsf{l}(1 : 0)$ is a minimal element, both terms on the l.h.s. of (2.17) are included in \mathcal{D} while the term on the r.h.s. is not, so (2.17) implies that there is no face \mathcal{F} of SAC_3 with $\mathcal{V}(\mathcal{F}) = \mathcal{D}$, and that for any face such that $\mathcal{V}(\mathcal{F}) = \mathcal{D}'$ with $\mathcal{D}' \supset \mathcal{D}$, we must have $\mathsf{l}(1 : 230) \in \mathcal{D}'$. Since $\mathsf{l}(1 : 230)$ is a maximal element, we are then forced to consider only down-sets that do not contain $\mathsf{l}(1 : 23)$. Permuting the parties in (2.17) to obtain analogous relations for the other elements of \mathcal{A} in (2.16), this implies that the only case that we need to consider is the one where \mathcal{D} is precisely the set of minimal elements. In fact, from (1.5) one can see that for $\mathbf{N} = 3$, $\dim(\mathcal{F}_*) = 1$, and for this choice of \mathcal{D} we get the ray generated by $\vec{S} = (1, 1, 1, 2, 2, 2, 1)$, which is an extreme ray and is the *only* KC-ER of SAC_3 . Therefore, in the simple case of $\mathbf{N} = 3$, the interplay of the constraints discussed in this section with the dependences among the MI instances reduces the size of the search space for the brute force strategy from 33,554,432 to 1! The combination of these constraints will indeed be a key aspect of the algorithm described in the next section.

Finally, let us conclude with another comment regarding the maximal elements of the MI-poset. For arbitrary \mathbf{N} , we can generalize (2.17) to be

$$\mathsf{l}(\underline{\mathcal{J}} : \underline{\mathcal{K}}) + \mathsf{l}(\underline{\mathcal{J}} : (\underline{\mathcal{K}})^c) = \mathsf{l}(\underline{\mathcal{J}} : \underline{\mathcal{J}}^c), \quad (2.18)$$

which shows that an arbitrary maximal element (on the r.h.s.) is a *positive* linear combination of other MI instances. Translating each MI in (2.18) to the corresponding SA, this shows that each SA instance corresponding to a maximal element of the poset is a *redundant inequality*, i.e., it is not a facet of the SAC_N . In other words, we could simply ignore all these SA instances and the cone would be exactly the same. However, for the sake of convenience in our algorithm, which we will explain below, we will instead choose to keep such redundant inequalities. Geometrically, we can interpret the set of redundant inequalities as specifying a “region” of the cone whose extreme rays we want to ignore. This will be another key element of the algorithm that we will now present.

3 The algorithm

In this section, we present the algorithm that we will use to find $\mathcal{R}_{\text{KC}}^6$. Since nothing about this algorithm is specific to the set-up of the subadditivity cone described in the previous section, we will present it more generally, such that it can be applied to other contexts without any adaptation. In general terms, our algorithm can be used when one has a polyhedral cone specified by a set of linear inequalities with partial order among them, and one wants to find only a particular subset of extreme rays, characterized by the fact that for each extreme ray the set of inequalities which are saturated is a down-set in the poset.²²

We anticipate that this algorithm is typically most useful in situations where the poset has “large height and small width.” In the limiting situation where the poset is a chain, our algorithm is very efficient (although somewhat trivial). In the opposite situation, where the poset is an antichain, it is instead very inefficient since it reduces to the brute force strategy mentioned in the Introduction, and one should instead use one of the standard algorithms for “polyhedral representation conversion” (although in general even these algorithms are not efficient) [26].²³ In intermediate situations, the efficiency will depend on the details of the problem at hand. Nevertheless, even for the specific problem of finding \mathcal{R}_{KC} indicated in the preceding section, where the height (approximately N) is exponentially smaller by a factor of roughly $2^D/\sqrt{N}$ than the width (approximately $\binom{N}{N/2}$), the algorithm remains remarkably useful. In any case, a feature of our algorithm is the flexibility of how it can be used in practice, and the possibility of easily combining it with another conversion algorithm. Essentially, one first runs our algorithm to extract a collection of lower-dimensional faces of the cone that is guaranteed to contain all the “down-set extreme rays.” Then one can find all the extreme rays for each of these faces using standard techniques and finally check which ones correspond to down-sets (which is a straightforward computation). Finally, we stress that even in this situation, the algorithm will provide useful information about “excluded regions” on the individual faces that in many cases can be used to simplify the derivation of the down-set extreme rays using standard conversion algorithms.

²² To make the algorithm more robust, we will make a few additional assumptions, which will be presented in detail below.

²³ Notice however that this inefficiency is related to the fact that the subset of extreme rays found by the algorithm becomes the full set of all extreme rays of the cone.

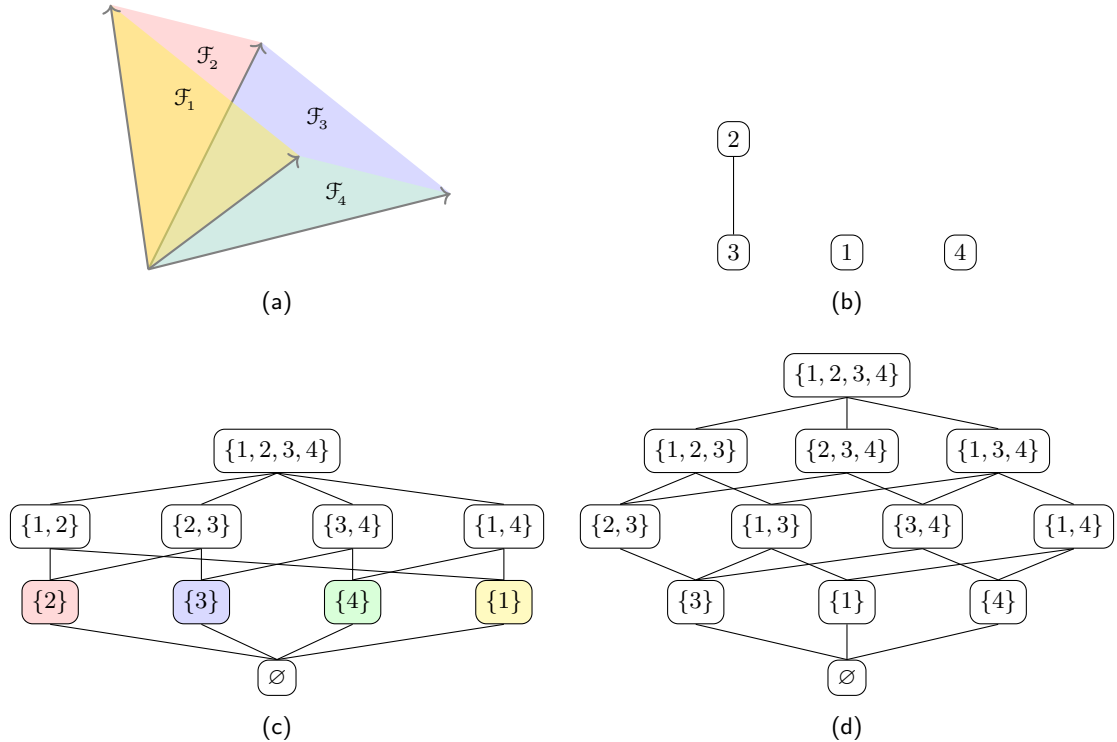


Figure 2: A 3-dimensional pointed cone \mathcal{C} in \mathbb{R}^3 specified by (a) a set of four (non-redundant) inequalities, (b) a choice of a poset \mathcal{P} for the inequalities, (c) the lattice of faces of \mathcal{C} , and (d) the lattice of down-sets of \mathcal{P} . The combinatorial automorphism groups are $G_{\mathcal{C}} \simeq D_4$ and $G_{\mathcal{P}} \simeq \mathbb{Z}_2$. Notice that $G_{\mathcal{P}} = \{e, (14)\}$ and is not a subgroup of $G_{\mathcal{C}}$, implying that $G_{\mathcal{C}} \wedge G_{\mathcal{P}} = \{e\}$. The D-ERs are $\{2, 3\}$, $\{3, 4\}$ and $\{1, 4\}$, whereas $\{1, 2\}$ is an ER but not a D-ER. On the other hand, the down-sets $\{3, 4\}$ and $\{1, 3\}$ belong to the same $G_{\mathcal{P}}$ -orbit, but $\{1, 3\}$ is not an ER.

3.1 Set-up

We begin by describing the set-up for our algorithm and by reviewing a few definitions and basic facts about polyhedral cones and systems of linear inequalities. For more details we refer the reader to standard references on the subject (e.g., see [27]). As a concrete and simple example of the set-up and the concepts introduced, we refer the reader to Figure 2.

Polyhedral cone: Consider a vector space \mathbb{R}^n , along with a finite collection of linear inequalities that specify a full-dimensional pointed cone \mathcal{C} .²⁴ We will write an inequality as $E_i(\vec{v}) \geq 0$, where E_i is an element of the dual space of \mathbb{R}^n and \vec{v} denotes an arbitrary vector in \mathbb{R}^n . Let \mathcal{E} denote the set of dual vectors E_i , with $i \in [k]$ and $k = |\mathcal{E}|$. A *face* \mathcal{F} of \mathcal{C} is defined as the intersection of \mathcal{C} with a hyperplane \mathbb{H} in \mathbb{R}^n such that \mathcal{C} is entirely contained in one of the two (closed) half-spaces specified by \mathbb{H} .²⁵ A codimension-1 face is

²⁴ Any cone specified by a finite set of inequalities is necessarily convex and polyhedral. If the cone is not full-dimensional we imagine to first “dimensionally reduce” the set-up to the subspace spanned by the cone. If it is not pointed, it is the Minkowski sum of a lower-dimensional cone and a linear subspace, and we can focus on this lower-dimensional cone.

²⁵ The full cone is also a face, obtained in the degenerate case where $E_i = \vec{0}$. In what follows we will ignore this face and always assume $E_i \neq \vec{0}$.

called a *facet*, and a 1-dimensional face an *extreme ray*.

In general, given an arbitrary collection of inequalities that specifies a full-dimensional pointed cone, it is not always the case that each inequality determines a facet. An inequality $E_i(\vec{v}) \geq 0$ such that \mathcal{F}_i is not a facet is called a *redundant inequality*. Geometrically, a redundant inequality $E_i(\vec{v}) \geq 0$ is characterized by the fact that for any $\vec{v}_* \in \mathcal{C}$ such that $E_i(\vec{v}_*) = 0$, we necessarily have $E_j(\vec{v}_*) = 0$ for some other E_j in \mathcal{E} . Algebraically, it is characterized by the fact that it is a *positive* linear combination of other inequalities in the set. Thus, if $E_i(\vec{v}) \geq 0$ is redundant, then the system of inequalities obtained by “ignoring” E_i (i.e., the set of inequalities specified by $\mathcal{E}' = \mathcal{E} \setminus \{E_i\}$) carves out the same cone \mathcal{C} . Given an arbitrary set of inequalities, one can use a linear program to check if a specific inequality is redundant. Indeed, there are efficient algorithms which reduce the set of inequalities to a minimum subset that specifies the same cone, where each inequality corresponds to a facet [28]. We therefore assume that each $E_i \in \mathcal{E}$ corresponds to a non-redundant inequality.²⁶

Poset: Having described the geometric structure of our set-up, we now assume that we further have a partial order among the elements of \mathcal{E} , and denote by $\mathcal{P} = (\mathcal{E}, \preceq)$ the resulting poset. For each face \mathcal{F} of \mathcal{C} , consider the subset $\mathcal{V}(\mathcal{F}) \subseteq \mathcal{E}$ associated to \mathcal{F} given by

$$\mathcal{V}(\mathcal{F}) = \{E_i \in \mathcal{E}, E_i(\vec{v}) = 0 \text{ for all } \vec{v} \in \text{int}(\mathcal{F})\}. \quad (3.1)$$

This is the subset of \mathcal{E} whose elements specify the inequalities which are saturated by the vectors in the interior of \mathcal{F} (notice that this set is independent from the choice of vector $\vec{v} \in \text{int}(\mathcal{F})$). If $\mathcal{V}(\mathcal{F})$ is a *down-set* in \mathcal{P} , we will say that \mathcal{F} is a *down-set face* (D-face). Our goal will be to find the 1-dimensional D-faces, or *down-set extreme rays* (D-ERs), of \mathcal{C} .²⁷

Symmetries: Our next assumption regards the symmetries that might be present in this set-up. Given a polyhedral cone, the set of its faces ordered by reverse inclusion²⁸ forms a lattice, which we shall call the face lattice $\mathcal{L}_{\mathcal{C}}$. Given (3.1), we can interpret each element of this lattice as the subset $\mathcal{V}(\mathcal{F})$. Consider now the group $\text{Sym}(k)$ of all possible permutations of \mathcal{E} , and its natural action on $\mathcal{L}_{\mathcal{C}}$. In general, an arbitrary element of this group does not preserve $\mathcal{L}_{\mathcal{C}}$. We call the largest subgroup $G_{\mathcal{C}} \leq \text{Sym}(k)$ of permutations that do preserve $\mathcal{L}_{\mathcal{C}}$ the *combinatorial automorphism group of the cone \mathcal{C}* [29].

Since the geometric and order structures of our set-up are independent from each other, an element of $G_{\mathcal{C}}$ in general might map a D-face to another face that is not a D-face. We assume now that the “structure” of the down-set corresponding to a D-face is important for the problem we want to solve with our algorithm,²⁹ so we want to consider the group of transformations that preserve this structure. To make this precise, we specify in what

²⁶ This assumption is mainly made here for the purpose of defining the cone and its symmetries. However, we will introduce certain redundant inequalities in §3.3 to specify a region of the cone that we want to ignore. This is why at the end of the previous section we chose to keep the maximal elements of the MI-poset.

²⁷ For the case where \mathcal{P} is the MI-poset, D-faces and D-ERs are precisely the KC-faces and KC-ERs, respectively.

²⁸ We use reverse inclusion rather than inclusion because it will be more convenient for comparison with another lattice that will be introduced momentarily. This is also the convention adopted in [6].

²⁹ Otherwise, there is no need to introduce the poset structure of \mathcal{E} in the first place.

sense two down-sets can be considered structurally equivalent. The set of down-sets of \mathcal{P} , ordered by inclusion, forms a lattice $\mathcal{L}_{\mathcal{P}}$, which we shall call the *down-set lattice* [25]. We define the *combinatorial automorphism group of the poset* $G_{\mathcal{P}}$ as the largest subgroup of $\text{Sym}(k)$ that preserves this lattice. Two down-sets of \mathcal{P} will be considered equivalent if they are related by such a permutation.

In general, $\mathcal{L}_{\mathcal{C}}$ and $\mathcal{L}_{\mathcal{P}}$, and therefore $G_{\mathcal{C}}$ and $G_{\mathcal{P}}$, are unrelated. Since we want to preserve both, we are then interested in the largest common subgroup

$$G_{\mathcal{C}\mathcal{P}} := G_{\mathcal{C}} \wedge G_{\mathcal{P}}. \quad (3.2)$$

For generic polyhedral cones and posets, it may however not be so easy to determine this group. Thus, in our algorithm below, we will simply assume we know a subgroup $G \leq G_{\mathcal{C}\mathcal{P}}$. The goal of the algorithm will then be to find all the D-ERs of \mathcal{C} only up to the action of G . Of course, there might exist a larger group G' , with $G \leq G' \leq G_{\mathcal{C}\mathcal{P}}$, and this would also preserve both the face and down-set lattices. Knowing G' would naturally lead to an increased efficiency of our algorithm, so we will take G as the largest such subgroup we can conveniently determine.

Excluded region: Finally, we also consider the possibility that in the problem we want to solve with our algorithm, we are only interested in finding the extreme rays that do not belong to a specified collection $\widehat{\mathcal{C}}$ of faces of \mathcal{C} . We will call $\widehat{\mathcal{C}}$ the *excluded region* of \mathcal{C} and assume that it is closed under the action of G . Specifically, each face $\mathcal{F} \in \widehat{\mathcal{C}}$ can be described by its corresponding set of saturated inequalities $\mathcal{V}(\mathcal{F})$, and using $\mathcal{V}(\mathcal{F})$ it is straightforward to close its orbit under the action of G .³⁰ While for a given specific problem the excluded region can be empty (no face is excluded), this notion, appropriately generalized to lower-dimensional faces, will play a key role during the computation. Since the algorithm proceeds by iteration, exploring at each step orbits of faces of various dimensionalities, we will use the excluded region to keep track of faces that have already been explored, or that are guaranteed to not include any new D-ER (more on this below), thereby allowing us to ignore them at subsequent steps of the computation.

3.2 Closure operators

As mentioned before, our strategy to find the D-ERs of \mathcal{C} will consist of scanning over the entire power-set $2^{\mathcal{E}}$ while ignoring most subsets $\mathcal{X} \subseteq \mathcal{E}$ that are either not down-sets or do not correspond to faces.³¹ Since the conditions for \mathcal{X} to be a down-set or a face correspond to two completely different and unrelated structures, namely the cone and the poset, we need a sufficiently general tool that “combines” both of these conditions and make the scan

³⁰ Notice that we are not making any assumption about the specific faces that appear in $\widehat{\mathcal{C}}$, and in general some of them can be facets. In this case it might be possible to simplify the problem by ignoring some of the inequalities to obtain a larger cone that is guaranteed to include all extreme rays of \mathcal{C} which are not in $\widehat{\mathcal{C}}$. We will further comment on this possibility in the next section, since in one variation of our algorithm we will apply this strategy to lower-dimensional faces generated during the computation.

³¹ In this subsection, we will ignore the symmetries and the excluded region $\widehat{\mathcal{C}}$; we will then combine all these ingredients in the following subsection.

over $2^{\mathcal{E}}$ more efficient. One such tool that will be key in our algorithm is the notion of a *closure operator*.

Definition 3. Given any set \mathcal{E} , a closure operator is a map $\text{cl} : 2^{\mathcal{E}} \rightarrow 2^{\mathcal{E}}$ such that, for any $\mathcal{X}, \mathcal{Y} \subseteq \mathcal{E}$, we have

- i) $\mathcal{X} \subseteq \text{cl}(\mathcal{X})$
- ii) $\mathcal{X} \subseteq \mathcal{Y} \implies \text{cl}(\mathcal{X}) \subseteq \text{cl}(\mathcal{Y})$
- iii) $\text{cl}(\text{cl}(\mathcal{X})) = \text{cl}(\mathcal{X})$.

A subset \mathcal{X} is said to be *closed* if $\text{cl}(\mathcal{X}) = \mathcal{X}$. Notice that from Definition 3, we can immediately derive the implication

$$\mathcal{X} \subseteq \mathcal{Y} \subseteq \text{cl}(\mathcal{X}) \implies \text{cl}(\mathcal{Y}) = \text{cl}(\mathcal{X}). \quad (3.3)$$

Indeed, taking the closure of all the terms on the l.h.s. of (3.3) and using the second property in Definition 3, we get $\text{cl}(\mathcal{X}) \subseteq \text{cl}(\mathcal{Y}) \subseteq \text{cl}(\text{cl}(\mathcal{X}))$. The third property then implies $\text{cl}(\mathcal{X}) \subseteq \text{cl}(\mathcal{Y}) \subseteq \text{cl}(\mathcal{X})$, from which (3.3) follows. This observation suggests that if we are only interested in closed subsets, and we can efficiently compute $\text{cl}(\mathcal{X})$ for any \mathcal{X} , then we might be able to scan over $2^{\mathcal{E}}$ more efficiently if for most \mathcal{X} there are “many” subsets \mathcal{Y} between \mathcal{X} and $\text{cl}(\mathcal{X})$.

In our set-up, we will consider three different closure operators.

1. *Down-set closure* (cl_D): For any given $\mathcal{X} \subseteq \mathcal{E}$, we define

$$\text{cl}_D(\mathcal{X}) = \{\mathbf{E}_i \in \mathcal{E}, \mathbf{E}_i \preceq \mathbf{E}_j \text{ for some } \mathbf{E}_j \in \mathcal{X}\}. \quad (3.4)$$

Clearly this is a closure operator according to Definition 3.

2. *Linear-dependence closure* (cl_L): For any given $\mathcal{X} \subseteq \mathcal{E}$, we define

$$\text{cl}_L(\mathcal{X}) = \{\mathbf{E}_i \in \mathcal{E}, \text{rank}(\mathcal{X} \cup \{\mathbf{E}_i\}) = \text{rank}(\mathcal{X})\}. \quad (3.5)$$

Again, this is a closure operator according to Definition 3.

3. *Face closure* (cl_F): The last closure operator that we introduce is more subtle. We will give a geometric definition, and refer the reader to [30] for more details and the proof that this definition indeed gives a closure operator (although intuitively this should already be quite clear from the geometric description). Let \mathbb{H}_i be the hyperplane consisting of the vectors \vec{v} satisfying the equality $\mathbf{E}_i(\vec{v}) = 0$. For any given $\mathcal{X} \subseteq \mathcal{E}$, let $\mathbb{V}_{\mathcal{X}}$ be the linear subspace of \mathbb{R}^n given by

$$\mathbb{V}_{\mathcal{X}} = \bigcap_{\mathbf{E}_i \in \mathcal{X}} \mathbb{H}_i, \quad (3.6)$$

and consider the face $\mathcal{F}_{\mathcal{X}} = \mathcal{C} \cap \mathbb{V}_{\mathcal{X}}$. Using (3.1) we define

$$\text{cl}_F(\mathcal{X}) = \mathcal{V}(\mathcal{F}_{\mathcal{X}}). \quad (3.7)$$

In other words, if the highest dimensional face \mathcal{F}_x contained in \mathbb{V}_x only spans a proper subspace of \mathbb{V}_x , then the face closure $\text{cl}_F(\mathcal{X})$ adds further elements from \mathcal{E} to reduce \mathbb{V}_x to this subspace.

Since we are neither interested in faces that are not D-faces nor in down-sets that do not correspond to faces, we want to compose these closure operators. Consider an arbitrary set \mathcal{E} and two distinct closure operators cl_1 and cl_2 . Notice that the composition $(\text{cl}_1 \circ \text{cl}_2)$ satisfies the first two conditions in Definition 3. Indeed, we have

$$\mathcal{X} \subseteq \text{cl}_2(\mathcal{X}) \subseteq \text{cl}_1(\text{cl}_2(\mathcal{X})) = (\text{cl}_1 \circ \text{cl}_2)(\mathcal{X}), \quad (3.8)$$

since both cl_1 and cl_2 are closure operators, thereby proving the first condition in Definition 3. Similarly,

$$\begin{aligned} \mathcal{X} \subseteq \mathcal{Y} &\implies \text{cl}_2(\mathcal{X}) \subseteq \text{cl}_2(\mathcal{Y}) \implies \text{cl}_1(\text{cl}_2(\mathcal{X})) \subseteq \text{cl}_1(\text{cl}_2(\mathcal{Y})) \\ &\implies (\text{cl}_1 \circ \text{cl}_2)(\mathcal{X}) \subseteq (\text{cl}_1 \circ \text{cl}_2)(\mathcal{Y}), \end{aligned} \quad (3.9)$$

which proves the second condition. However, $(\text{cl}_1 \circ \text{cl}_2)$ is in general not a closure operator because it does not satisfy the third condition in Definition 3, as $\text{cl}_2(\mathcal{X})$ is not necessarily a closed set with respect to cl_1 .³²

Consider now the operator $(\text{cl}_1 \circ \text{cl}_2)^t$, defined by applying t iterations of $(\text{cl}_1 \circ \text{cl}_2)$. Each application of $(\text{cl}_1 \circ \text{cl}_2)$ either augments the previous set by some element, or it preserves the set. In the latter case, further applications of $(\text{cl}_1 \circ \text{cl}_2)$ do not do anything since the set is already closed, whereas in the former case, the maximum number of augmentations is obviously bounded by the cardinality of the set (although typically this bound is far from being saturated). Therefore, if we define

$$\begin{aligned} \text{cl}_{12} : 2^{\mathcal{E}} &\rightarrow 2^{\mathcal{E}} \\ \mathcal{X} &\mapsto (\text{cl}_1 \circ \text{cl}_2)^{|\mathcal{E}|}(\mathcal{X}), \end{aligned} \quad (3.10)$$

it then follows that cl_{12} is a closure operator. In the next section, we will consider the following closure operators, obtained in this way by combining cl_F and cl_L with cl_D , so that

$$\begin{aligned} \text{cl}_{FD} &:= (\text{cl}_F \circ \text{cl}_D)^{|\mathcal{E}|} \\ \text{cl}_{LD} &:= (\text{cl}_L \circ \text{cl}_D)^{|\mathcal{E}|}. \end{aligned} \quad (3.11)$$

We will use the first operator cl_{FD} to formulate the algorithm in terms of faces of the cone. The second operator cl_{LD} will instead appear in the variation of the algorithm, discussed in §3.4, which we actually used to derive the results presented in §4 and §5. We are now ready to describe the algorithm in detail.

³² As a simple example, consider a poset \mathcal{P} such that there is no element which is incomparable with every other element. Let $\text{cl}_1 = \text{cl}_D$ as defined above, and $\text{cl}_2 = \text{cl}_U$, where cl_U is the *up-set* closure operator defined analogously to cl_D where we simply replace \preceq with \succeq in (3.4). Then the only subset $\mathcal{X} \subseteq \mathcal{P}$ which is closed under both cl_1 and cl_2 is $\mathcal{X} = \mathcal{P}$.

3.3 The algorithm in detail

We first specify the main ingredients of the algorithm and list the key steps to orient the reader. Subsequently, when we prove the completeness of the algorithm (Theorem 2), we explain its logic and the rationale behind its construction.

The computation will be organized in terms of certain D-faces of \mathcal{C} which will be found by intermediate steps of the algorithm. However, since our goal is to compute just the D-ERs, each belonging to multiple faces, only some D-faces will be determined by the algorithm (which D-faces in particular will depend on different choices made during the computation, devised such that the chosen collection contains all the D-ERs). Each D-face \mathcal{F} will be associated to a triplet of the form $\mathfrak{T} = (\mathcal{D}, \mathcal{U}, G_{\mathcal{D}})$, where $\mathcal{D} = \mathcal{V}(\mathcal{F})$, $G_{\mathcal{D}}$ is the subgroup of G that *stabilizes* \mathcal{D} ,³³ and $\mathcal{U} \subseteq \mathcal{E}$ is an *up-set* specifying an excluded region $\widehat{\mathcal{F}}$ on the boundary of \mathcal{F} as follows. To each $E_i \in \mathcal{U}$, we associate the hyperplane

$$\mathbb{H}_i = \{\vec{v} \in \mathbb{R}^n, E_i(\vec{v}) = 0\}. \quad (3.12)$$

This hyperplane specifies a face \mathcal{F}_i on the boundary of \mathcal{F} via

$$\mathcal{F}_i = \mathbb{H}_i \cap \mathcal{F}. \quad (3.13)$$

Given \mathcal{U} , we then define the excluded region of \mathcal{F} as the collection of faces

$$\widehat{\mathcal{F}} = \{\mathcal{F}_i, E_i \in \mathcal{U}\}. \quad (3.14)$$

Notice that while in §3.1 we characterized a face in the excluded region of the cone $\widehat{\mathcal{C}}$ by the set $\mathcal{V}(\mathcal{F})$, here we are instead specifying each element of $\widehat{\mathcal{F}}$ (which is also a face of \mathcal{C}) via the saturation of a single inequality. The equivalence of these descriptions will become evident momentarily, when we describe the initialization of the algorithm and explain how by introducing certain redundant inequalities we can translate the description of $\widehat{\mathcal{C}}$ into the language that we are using here.

The algorithm is initialized with one of these triplets. The *main subroutine* then “processes” this triplet and outputs a set of new triplets which are “simpler” in a sense that we will clarify below, and possibly some D-ERs. We then repeat this procedure until a certain criterion is met. This criterion is specified during the initialization and allows for some flexibility in how the algorithm can be used in practice. A schematic description of the algorithm is shown in Algorithm 1, and we now describe each component in detail.

Initialization: The algorithm begins with a triplet $\mathfrak{T}^{(0)} = (\mathcal{D}^{(0)}, \mathcal{U}^{(0)}, G^{(0)})$ corresponding to the set-up described in §3.1. The face \mathcal{F}_0 is the full cone \mathcal{C} , which corresponds to $\mathcal{D}^{(0)} = \emptyset$; $G^{(0)} = G$ is the subgroup of $G_{\mathcal{CP}}$ that we assume to be known explicitly; and $\mathcal{U}^{(0)}$ corresponds to a new set of *redundant* inequalities which conveniently specifies the excluded region $\widehat{\mathcal{C}}$ of the cone, and is constructed as follows. As explained before, each face $\mathcal{F}_i \in \widehat{\mathcal{C}}$ is described by the set $\mathcal{V}(\mathcal{F}_i)$, which we can use to construct the dual vector

$$E_i = \sum_{E_j \in \mathcal{V}(\mathcal{F}_i)} \sigma_j E_j, \quad (3.15)$$

³³This is the *stabilizer group* of \mathcal{D} , i.e., the subgroup of G of elements that leave \mathcal{D} unchanged.

Algorithm 1: Global structure of the algorithm

input : the initial triplet $\mathfrak{T}^{(0)} = (\mathcal{D}^{(0)}, \mathcal{U}^{(0)}, G^{(0)})$
 $f(\mathfrak{T}, \lambda)$ in Function 1 used to stop the computation
 $g(\mathfrak{T})$ in Function 2 used by the main subroutine to generate new triplets
output: a set \mathfrak{T} of triplets such that Condition 1 holds and $f(\mathfrak{T}, \lambda) = \text{TRUE}$
 a set \mathfrak{R} of D-ERs

$\mathfrak{T} \leftarrow \{\mathfrak{T}^{(0)}\};$
 $\mathfrak{R} \leftarrow \emptyset;$
while $\exists \mathfrak{T} \in \mathfrak{T}$ such that $f(\mathfrak{T}, \lambda) = \text{FALSE}$ **do**
 run the main subroutine (Algorithm 2) on the first $\mathfrak{T} \in \mathfrak{T}$ such that
 $f(\mathfrak{T}, \lambda) = \text{FALSE};$
 update \mathfrak{T} by deleting $\mathfrak{T};$
 add to \mathfrak{T} the new triplets in the output of the main subroutine;
 add to \mathfrak{R} any new D-ER in the output of the main subroutine;

for some choice of $\sigma_j \in \mathbb{R}^+$. Since this is a positive linear combination, the inequality $E_i(\vec{v}) \geq 0$ is redundant, and it is saturated only by vectors that saturate all inequalities $E_j(\vec{v}) \geq 0$ for $E_j \in \mathcal{V}(\mathcal{F}_i)$. Equivalently, this means that if we let \mathbb{H}_i be the hyperplane specified by E_i as in (3.12), we have $\mathcal{F}_i = \mathbb{H}_i \cap \mathcal{C}$. This is convenient because it allows us to treat the excluded region $\widehat{\mathcal{C}}$ of \mathcal{C} in the same way as we treat the excluded region $\widehat{\mathcal{F}}$ of a D-face \mathcal{F} obtained at an intermediate stage of the computation. In terms of the poset structure, there are many ways to extend the poset \mathcal{E} to include these new dual vectors E_i (one for each $\mathcal{F}_i \in \widehat{\mathcal{C}}$). The simplest is to just have the redundant E_i form an antichain that is “wholly disjoint” from the rest of the poset,³⁴ although it is oftentimes natural to add the redundant E_i “at the top” of the original poset.³⁵ In this case, a simple solution that is guaranteed to preserve the symmetry of the problem is to specify cover relations such that each new E_i covers every maximal element of the original poset. However, this is not strictly necessary, and in specific situations other extensions might be more natural.³⁶ Importantly, regardless of how we choose to extend the poset with the new dual vectors, while the full set of D-ERs of \mathcal{C} might change because of the extension, the set of D-ERs which are not in $\widehat{\mathcal{C}}$ remains unchanged.

In addition to the initial triplet $\mathfrak{T}^{(0)}$, the initialization of the algorithm also requires the specification of a function that will be used to stop the computation. Denoting by \mathfrak{T} an arbitrary triplet generated during the computation, we define this function as follows.

Function 1. A Boolean function $f(\mathfrak{T}, \lambda)$, fixed for all triplets, which returns TRUE if a chosen set of attributes of \mathfrak{T} (which enter into the definition of f) satisfies a set of constraints parametrized by λ .

³⁴ By this we mean that each E_i is incomparable to any other element in the poset.

³⁵ By this we mean that each E_i covers some other element of the poset but is not covered by any element.

³⁶ For example, in the case of the MI-poset, the only redundant inequalities are precisely the ones given by the entropies “at the top” of the poset, and they specify part of the excluded region.

Typically, f will be a function that can be computed efficiently from the data given by a triplet, and should be chosen depending on the specific details of the problem to which the algorithm is applied. One useful example of this function is an upper bound to the dimension of the face corresponding to the triplet \mathfrak{T} , where f returns TRUE if the bound is satisfied and FALSE otherwise. If one wants to use the algorithm to *directly* find all G -orbits of D-ERs of \mathcal{C} which are not in $\widehat{\mathcal{C}}$, then one can simply set this bound to 1. Another option instead is to set a larger upper bound for the dimension of a face, and use the algorithm to restrict the search space to a point where one can then use other methods to find the extreme rays of the resulting lower-dimensional faces. An alternative option that might be useful is to stop the computation only when the excluded region on a face is sufficiently vast.³⁷

Finally, at this stage one should also choose a function g to specify another criterion (see Function 2 below), which will be used at each iteration by the main subroutine to generate new triplets given one triplet as input. As we will explain, the choice of this function affects which D-faces are found by the algorithm at intermediate steps of the computation, and different choices might make a significant difference in terms of efficiency.

Main subroutine: The main subroutine is the core of our algorithm. The input is a triplet $\mathfrak{T} = (\mathcal{D}, \mathcal{U}, G_{\mathcal{D}})$, corresponding to a face \mathcal{F} , that satisfies Condition 1 outlined below. During the computation, new triplets will be generated which do not necessarily satisfy these conditions. Some of these triplets will correspond to D-ERs and will be stored, while the others will be either discarded or modified such that the conditions are satisfied. The triplets in the output correspond to a simplification of the problem because for each one of them, either the down-set strictly contains \mathcal{D} , and therefore the dimension of the corresponding face is smaller than that of \mathcal{F} , or the excluded region is strictly larger, therefore reducing the set of lower-dimensional faces that we still need to consider in our search of D-ERs. Furthermore, most new triplets have both of these properties.

We now describe the conditions that we require for each triplet and the corresponding face. By our assumptions about the set-up described in §3.1, it is trivial to check that the triplet $\mathfrak{T}^{(0)}$ used to initialize the algorithm satisfies these conditions.³⁸

Condition 1. *Given a triplet $\mathfrak{T} = (\mathcal{D}, \mathcal{U}, G_{\mathcal{D}})$ corresponding to a face \mathcal{F} and excluded region $\widehat{\mathcal{F}}$, we require*

- i) $\mathcal{D} \cap \mathcal{U} = \emptyset$*
- ii) $\dim(\mathcal{F}) > 1$*
- iii) \mathcal{U} is stabilized by $G_{\mathcal{D}}$*
- iv) $\dim(\mathcal{F}) = \text{rank}(\mathcal{E} \setminus (\mathcal{D} \cup \mathcal{U})|_{\mathcal{F}})$*

The first condition ensures that the excluded region $\widehat{\mathcal{F}}$ on \mathcal{F} is not the entire face. The second condition demands that \mathcal{F} is not a D-ER. The third condition ensures that if a D-ER is in the excluded region $\widehat{\mathcal{F}}$, then any other D-ER in the same $G_{\mathcal{D}}$ -orbit is also excluded. Finally, the last condition deserves a more careful explanation. Suppose we have a D-face

³⁷ We will use the first option to obtain the results presented in §4 and a combination of the latter two to obtain the results presented in §5.

³⁸ This is true except for trivial situations, such as the case where \mathcal{C} is 1-dimensional, which we ignore.

Algorithm 2: The main subroutine

input : a triplet $\mathfrak{T} = (\mathcal{D}, \mathcal{U}, G_{\mathcal{D}})$ that satisfies Condition 1
output: a set $\check{\mathfrak{T}}$ of triplets that satisfy Condition 1
 a set \mathfrak{K} of D-ERs

$\mathcal{M} \leftarrow$ the maximal elements of $\mathcal{E} \setminus (\mathcal{D} \cup \mathcal{U})$;
 $\mathfrak{M} \leftarrow$ the partition of \mathcal{M} into $G_{\mathcal{D}}$ -orbits;
 $\mathfrak{D} \leftarrow \emptyset$;
for each orbit $\mathcal{M}_m \in \mathfrak{M}$ **do**
 choose an arbitrary element E_m of the orbit \mathcal{M}_m ;
 $\mathcal{D}_m \leftarrow \text{cl}_{\text{FD}}(\mathcal{D} \cup \{E_m\})$;
 append \mathcal{D}_m to \mathfrak{D} ;
 1 $\bar{\mathcal{U}} \leftarrow$ the union of \mathcal{U} and all orbits \mathcal{M}_m of \mathfrak{M} such that $\mathcal{D}_m \cap \mathcal{U} \neq \emptyset$;
 $\dot{\mathfrak{D}} \leftarrow \{\mathcal{D}_m \in \mathfrak{D}, \mathcal{D}_m \cap \mathcal{U} = \emptyset\}$;
 $\dot{\mathfrak{M}} \leftarrow \{\mathcal{M}_m \in \mathfrak{M}, \mathcal{D}_m \cap \mathcal{U} = \emptyset\}$;
 for each $\mathcal{D}_m \in \dot{\mathfrak{D}}$ **do**
 if the face \mathcal{F}_m is 1-dimensional **then**
 add \mathcal{F}_m to \mathfrak{K} ;
 delete \mathcal{D}_m from $\dot{\mathfrak{D}}$;
 add all elements of \mathcal{M}_m to $\bar{\mathcal{U}}$;
 delete \mathcal{M}_m from $\dot{\mathfrak{M}}$;
 2 $(\ddot{\mathfrak{D}}, \ddot{\mathfrak{M}}) \leftarrow$ the output of the subroutine in Algorithm 3 run on $(\dot{\mathfrak{D}}, \dot{\mathfrak{M}})$;
 3 $\mathfrak{C} \leftarrow$ the output of the subroutine in Algorithm 4 run on $(\ddot{\mathfrak{D}}, \ddot{\mathfrak{M}})$;
 4 $\check{\mathfrak{T}} \leftarrow$ the output of the subroutine in Algorithm 5 run on \mathfrak{C} ;
 5 append to $\check{\mathfrak{T}}$ the triplet $(\mathcal{D}, \mathcal{U} \cup \mathcal{M}, G_{\mathcal{D}})$;
 $\check{\mathfrak{T}} \leftarrow \emptyset$;
 6 **for** each $\mathfrak{T} \in \check{\mathfrak{T}}$ **do**
 if $\dim(\mathcal{F}) - \text{rank}(\mathcal{E} \setminus (\mathcal{D} \cup \mathcal{U})|_{\mathcal{F}}) = 0$ **then**
 | add \mathfrak{T} to $\check{\mathfrak{T}}$;
 else
 | **if** $\dim(\mathcal{F}) - \text{rank}(\mathcal{E} \setminus (\mathcal{D} \cup \mathcal{U})|_{\mathcal{F}}) = 1$ **then**
 | if $\mathcal{E} \setminus \mathcal{U} = \mathcal{V}(\mathcal{F})$ for some $\mathcal{F} \notin \hat{\mathcal{C}}$, add \mathfrak{T} to \mathfrak{K} ;
 7

\mathcal{F} , with $\mathcal{V}(\mathcal{F}) = \mathcal{D}$, and an excluded region $\hat{\mathcal{F}}$ specified by \mathcal{U} . Since we are only interested in finding D-ERs in \mathcal{F} outside of $\hat{\mathcal{F}}$, we only care about ERs that do not saturate any of the inequalities specified by \mathcal{U} . We denote by $\mathcal{E} \setminus (\mathcal{D} \cup \mathcal{U})|_{\mathcal{F}}$ the reduction of the inequalities specified by the set $\mathcal{E} \setminus (\mathcal{D} \cup \mathcal{U})$ to the linear subspace spanned by \mathcal{F} . The last condition then demands that the cone specified by these inequalities in the subspace spanned by \mathcal{F} is a pointed cone.

The computation of the main subroutine is presented in full in Algorithm 2. Here

Algorithm 3: Checking the equivalence of faces under $G_{\mathcal{D}}$

input : a collection $\dot{\mathcal{D}}$ of down-sets, each one corresponding to a face
a collection $\dot{\mathcal{M}}$ of subsets of \mathcal{M} , one for each down-set in $\dot{\mathcal{D}}$
the group $G_{\mathcal{D}}$ from the computation in the main subroutine
output: a subset $\ddot{\mathcal{D}}$ of $\dot{\mathcal{D}}$ whose elements belong to distinct $G_{\mathcal{D}}$ -orbits
a new collection $\ddot{\mathcal{M}}$ of subsets of \mathcal{M} , one for each down-set in $\ddot{\mathcal{D}}$

$\ddot{\mathcal{D}} \leftarrow \emptyset;$

$\ddot{\mathcal{M}} \leftarrow \emptyset;$

$\mathcal{O} \leftarrow$ the partition of $\dot{\mathcal{D}}$ into $G_{\mathcal{D}}$ -orbits;

for each orbit in \mathcal{O} **do**

append to $\ddot{\mathcal{D}}$ an arbitrary representative of the orbit;

append to $\ddot{\mathcal{M}}$ the union of all \mathcal{M}_m in $\dot{\mathcal{M}}$ corresponding to the down-sets \mathcal{D}_m in the orbit;

we clarify some of the steps, describe the internal subroutines presented in Algorithm 3, Algorithm 4, and Algorithm 5, and present a few possible choices for the function g which affects the output at each iteration. The numbers in the numbered list below refer to corresponding lines in Algorithm 2.

- 1) After constructing $\bar{\mathcal{U}}$, one may wonder if the efficiency of the algorithm can be improved by further checking whether there is some $\mathcal{D}_m \in \dot{\mathcal{D}}$ such that $\mathcal{D}_m \cap \bar{\mathcal{U}} \neq \emptyset$ while $\mathcal{D}_m \cap \mathcal{U} = \emptyset$, in which case one could add more elements to $\bar{\mathcal{U}}$ and extend the excluded region for the new triplets that will be constructed in the following steps. However, this is not the case due to the following implication:³⁹

$$\mathcal{D}_m \cap \mathcal{U} = \emptyset \implies \mathcal{D}_m \cap \bar{\mathcal{U}} = \emptyset \quad \text{for all } \mathcal{D}_m \in \dot{\mathcal{D}}. \quad (3.16)$$

- 2) The goal of Algorithm 3 is to check if some of the faces corresponding to the triplets in $\dot{\mathcal{D}}$ are related by an element of $G_{\mathcal{D}}$. (Although this would not be the case for the generating elements \mathcal{M}_m themselves by construction, the enlargement from using cl_{FD} can subsequently enhance the symmetry.) In that case, there is no reason to further process each equivalent triplet, and we simply select one. Furthermore, for each value of the index m , we combine all elements of each $\mathcal{M}_{m'}$ with $\mathcal{D}_{m'} \sim \mathcal{D}_m$ into a single new set. The resulting subsets of \mathcal{M} will be used to generate the excluded regions of the new faces, as explained below.
- 3) Algorithm 4 generates a collection of new triplets starting from the output of Algorithm 3. It relies on the function $g(\mathcal{D}_m, \mathcal{M}_m)$, which has to be chosen at the initialization, to reorder the elements of $\dot{\mathcal{D}}$ and $\dot{\mathcal{M}}$.

³⁹ We can argue this as follows. Let $\mathcal{D}_m = \text{cl}_{\text{FD}}(\mathcal{D} \cup \{\mathbf{E}_m\})$ for some \mathbf{E}_m , and suppose \mathcal{D}_m contains an element $\mathbf{E}_{m'} \in \mathcal{M}_{m'}$ for some $\mathcal{M}_{m'} \subseteq \bar{\mathcal{U}} \setminus \mathcal{U}$. Then $\mathcal{D}_{m'} = \text{cl}_{\text{FD}}(\mathcal{D} \cup \{\mathbf{E}_{m'}\})$ by construction intersects \mathcal{U} , i.e., $\exists \mathbf{U} \in \mathcal{U} \cap \mathcal{D}_{m'}$. Hence, since $\mathbf{E}_{m'} \in \mathcal{D}_m$, it follows from fundamental properties of closure operators that $\mathcal{D}_m = \text{cl}_{\text{FD}}(\mathcal{D} \cup \{\mathbf{E}_m\}) \supseteq \text{cl}_{\text{FD}}(\mathcal{D} \cup \{\mathbf{E}_{m'}\}) \ni \mathbf{U}$. In other words, \mathcal{D}_m would have also intersected \mathcal{U} .

Algorithm 4: Generating the triplets

input : the collection $\mathring{\mathfrak{D}}$ of down-sets from the output of Algorithm 3
 the collection $\mathring{\mathfrak{M}}$ of subsets of \mathcal{E} from the output of Algorithm 3
 the set $\overline{\mathcal{U}}$ from the computation in the main subroutine
 the Function 2 chosen at initialization
output: a collection \mathfrak{T} of triplets
 $\mathfrak{T} \leftarrow \emptyset$;
 reorder the elements of $\mathring{\mathfrak{D}}$ and $\mathring{\mathfrak{M}}$ using Function 2 (see main text);
 index the elements of these sequences by $q \in \{1, 2, \dots, Q\}$ (this fixes \mathcal{D}_q and \mathcal{M}_q);
 $\mathcal{M}_0 \leftarrow \emptyset$;
 $\mathcal{U}_0 \leftarrow \overline{\mathcal{U}}$;
for each q **do**
 $\mathcal{U}_q \leftarrow \mathcal{U}_{q-1} \cup \mathcal{M}_{q-1}$;
 compute the stabilizer group $G_{\mathcal{D}_q}$ of \mathcal{D}_q ;
 append the triplet $\mathfrak{T}_q = (\mathcal{D}_q, \mathcal{U}_q, G_{\mathcal{D}_q})$ to \mathfrak{T} ;

Function 2. A vector-valued function $g(\mathcal{D}_m, \mathcal{M}_m)$, which is fixed for all pairs and can be easily computed.

The algorithm orders the elements $\mathcal{D}_m \in \mathring{\mathfrak{D}}$ and $\mathcal{M}_m \in \mathring{\mathfrak{M}}$ such that the value of the first component of the output of Function 2 is non-decreasing along the sequence. It then orders the elements \mathcal{D}_m and \mathcal{M}_m with the same value of the first component of Function 2 according to the second component (again such that this is non-increasing), and so on. Depending on the details of the problem, different choices might have a decisive effect on the efficiency of the algorithm. Examples of the attributes computed by $g(\mathcal{D}_m, \mathcal{M}_m)$ can be the dimension of the corresponding face, or the cardinality of the corresponding down-set.

- 4) Notice that at this stage of the main subroutine each triplet in the output of Algorithm 4 already satisfies (i) and (ii) in Condition 1, since the former is implemented by the definition of $\mathring{\mathfrak{D}}$, and the latter by saving 1-dimensional faces into \mathfrak{R} and deleting the corresponding down-sets from $\mathring{\mathfrak{D}}$ even before running Algorithm 3. Algorithm 5 first implements (iii) in Condition 1 for each triplet by completing the orbit of \mathcal{U}_q under the action of $G_{\mathcal{D}_q}$. It then attempts to “extend” the excluded regions by checking which elements in $\mathcal{E} \setminus (\mathcal{D}_q \cup \mathcal{U}_q)$ would, after adding them to \mathcal{D}_q and taking the closure, generate an element in \mathcal{U}_q . By doing so using orbits of $G_{\mathcal{D}_q}$, it is guaranteed that the new updated triplets in the output also satisfy (iii) in Condition 1.
- 5) The main goal of the main subroutine is to generate new triplets by adding at least one new element from \mathcal{M} to \mathcal{D} . However, we should also take into account the case where no such element is added to \mathcal{D} . We can then add all the elements of \mathcal{M} to the excluded region.

Algorithm 5: Updating the triplets

input : the collection \mathfrak{T} of triplets from the output of Algorithm 4

output: a collection $\check{\mathfrak{T}}$ of triplets that satisfies (iii) in Condition 1

$\check{\mathfrak{T}} \leftarrow \emptyset$;

for each triplet $\mathfrak{T}_q = (\mathcal{D}_q, \mathcal{U}_q, G_{\mathcal{D}_q})$ in \mathfrak{T} **do**

update \mathcal{U}_q by completing its orbit under the action of $G_{\mathcal{D}_q}$;

partition $\mathcal{E} \setminus (\mathcal{D}_q \cup \mathcal{U}_q)$ into $G_{\mathcal{D}_q}$ orbits;

for each orbit **do**

choose a representative E_k ;

if $\text{cl}_{\text{FD}}(\mathcal{D}_q \cup \{E_k\}) \cap \mathcal{U} \neq \emptyset$ **then**

add all the elements of the orbit to \mathcal{U}_q

-
- 6) Each triplet in $\check{\mathfrak{T}}$ satisfies the first three requirements of Condition 1. At this step, we check which triplets in $\check{\mathfrak{T}}$ satisfy the last requirement, and include them as part of the final output $\check{\check{\mathfrak{T}}}$.
- 7) If a triplet in $\check{\mathfrak{T}}$ does not satisfy (iv) in Condition 1, we have to distinguish two cases. If

$$\dim(\mathcal{F}) - \text{rank}(\mathcal{E} \setminus (\mathcal{D} \cup \mathcal{U})|_{\mathcal{F}}) = 1, \quad (3.17)$$

it is possible that by further saturating all the inequalities specified by the elements of $\mathcal{E} \setminus \mathcal{U}$ we obtain a subspace spanned by a D-ER which is not in $\widehat{\mathcal{C}}$, and in that case we add it to the output. On the other hand, if

$$\dim(\mathcal{F}) - \text{rank}(\mathcal{E} \setminus (\mathcal{D} \cup \mathcal{U})|_{\mathcal{F}}) > 1, \quad (3.18)$$

the inequalities specified by the elements of $\mathcal{E} \setminus (\mathcal{D} \cup \mathcal{U})$ are not enough to carve out a pointed cone in the subspace spanned by \mathcal{F} . This means that any ER on \mathcal{F} is necessarily in $\widehat{\mathcal{C}}$, and we can discard the triplet entirely.

Proof of completeness: We now prove that for an arbitrary set-up as described in §3.1, our algorithm gives all the D-ERs which are not in the excluded region.

Theorem 2. For each down-set extreme ray $\vec{\mathcal{F}}$ of the cone \mathcal{C} which is not in the excluded region $\widehat{\mathcal{C}}$, at least one of the following is true:

- The set \mathfrak{R} contains at least one element of the G -orbit of $\vec{\mathcal{F}}$.
- The set $\check{\mathfrak{T}}$ contains at least one higher-dimensional face \mathcal{F} such that at least one representative of the G -orbit of $\vec{\mathcal{F}}$ is in \mathcal{F} and not in $\widehat{\mathcal{F}}$.

Proof. As we mentioned before, the basic idea of the algorithm is to essentially scan over the entire space of all possible down-sets of the MI-poset and check which down-sets are D-ERs. To make this scan more efficient, we will use various constraints to ignore most

down-sets, and we will prove below that these constraints do not miss any relevant ones. Since the full algorithm (see Algorithm 1) is simply an iteration of the main subroutine in Algorithm 2, we only need to show the statement of the theorem for a single iteration, i.e., we only need to show that given a triplet \mathfrak{T} corresponding to a face \mathcal{F} and an arbitrary D-ER $\vec{\mathcal{F}} \in \mathcal{F}$ not in the excluded region $\widehat{\mathcal{F}}$ of \mathcal{F} , the output of the main subroutine includes at least one element in the $G_{\mathcal{D}}$ -orbit of $\vec{\mathcal{F}}$.

We begin with setting $\mathcal{D} = \mathcal{V}(\mathcal{F})$, and notice that for any D-ER $\vec{\mathcal{F}} \in \mathcal{F}$, we have $\mathcal{V}(\vec{\mathcal{F}}) \supseteq \mathcal{D}$. This means our algorithm should scan over all possible \mathcal{D}' such that $\mathcal{D}' \supseteq \mathcal{D}$. However, since we are not interested in any ER in $\widehat{\mathcal{F}}$, we can impose the constraint $\mathcal{U} \cap \mathcal{D}' = \emptyset$, so that it suffices to consider all possible deformations of \mathcal{D} obtained by adding to it elements from an arbitrary subset of $\mathcal{E} \setminus (\mathcal{D} \cup \mathcal{U})$. We will do so element by element, taking advantage of closure operators, the symmetries of the problem, and the poset structure.

Importantly, we do not consider all these possibilities in a single iteration of the main subroutine. Instead, to take advantage of the poset structure, in a single iteration we only consider the down-sets obtained by adding to \mathcal{D} an element of \mathcal{M} , which is the set of maximal elements of $\mathcal{E} \setminus (\mathcal{D} \cup \mathcal{U})$. More precisely, we organize all possible down-sets \mathcal{D}' into two families: Those that include at least one element of \mathcal{M} , and those that do not. The down-sets in the second family are collected in a new triplet $(\mathcal{D}, \mathcal{U} \cup \mathcal{M}, G_{\mathcal{D}})$ (see line 5 in Algorithm 2) and will be processed at a later iteration. Therefore, we only need to show that the procedure in Algorithm 2 guarantees a complete scan over the first family.

Consider an element $E \in \mathcal{M}$ and the set $\mathcal{D} \cup \{E\}$. If there is another element E' which is mapped to E by an element of the stabilizer group $G_{\mathcal{D}}$ of \mathcal{D} , then clearly $\mathcal{D} \cup \{E\}$ and $\mathcal{D} \cup \{E'\}$ are related by the same group operation. Therefore, since we are only interested in finding D-ERs up to equivalence under the action of $G_{\mathcal{D}}$, once we include in the scan the down-sets obtained from \mathcal{D} by adding E , we can ignore any down-set obtained from \mathcal{D} by adding E' . We then partition \mathcal{M} into $G_{\mathcal{D}}$ -orbits and focus only on deformations of \mathcal{D} generated by representatives of these orbits. This partition of \mathcal{M} is denoted by \mathfrak{M} .

The set $\mathcal{D} \cup \{E\}$ does not necessarily correspond to a new D-face of the cone, and to obtain such a face we compute $\text{cl}_{\text{FD}}(\mathcal{D} \cup \{E\})$. As explained in §3.2, we can then ignore any down-set \mathcal{D}'' such that $\mathcal{D} \cup \{E\} \subset \mathcal{D}'' \subset \text{cl}_{\text{FD}}(\mathcal{D} \cup \{E\})$ (cf. (3.3)). Computing the closure for an arbitrary representative from every component in \mathfrak{M} , we obtain a set \mathfrak{D} of down-sets, each of which corresponding to a D-face. Up to this point, it should be clear that the procedure guarantees completeness, in the sense that any D-ER of \mathcal{F} not in $\widehat{\mathcal{F}}$ is either (i) in one of these faces corresponding to a down-set in \mathfrak{D} ; (ii) in another D-face that is related to a down-set in \mathfrak{D} by the action of $G_{\mathcal{D}}$; or (iii) in a D-face whose down-set does not include any element of \mathcal{M} (and will therefore be processed at a later iteration). The rest of the proof then focuses on demonstrating that the additional steps in the main subroutine used to increase the efficiency of our algorithm, namely ignoring certain elements of \mathfrak{D} and producing the triplets (including new excluded regions) for the remaining ones, do not miss any relevant D-ERs.

Starting from \mathcal{U} , we now construct a new set $\overline{\mathcal{U}}$ of elements that we will use to specify the excluded region of the new faces. First, notice that a new face corresponding to an element in \mathfrak{D} might already be entirely contained in the excluded region $\widehat{\mathcal{F}}$ of the initial

face \mathcal{F} , i.e., if $\text{cl}_{\text{FD}}(\mathcal{D} \cup \{\mathbf{E}\}) \cap \mathcal{U} \neq \emptyset$, in which case they can be ignored. If this is true, we add all elements in the orbit of \mathbf{E} to $\bar{\mathcal{U}}$, since we do not want to add \mathbf{E} (or any equivalent element) to the down-set of any lower-dimensional face that we derive from \mathcal{F} . Furthermore, some elements of \mathfrak{D} might already correspond to D-ERs, in which case we add them to \mathfrak{K} and again add all the elements in the orbit of \mathbf{E} to $\bar{\mathcal{U}}$, since adding any further element beyond \mathbf{E} would only yield the trivial dimensional space. After these steps, we are left with a sub-collection of D-faces \mathfrak{D} and orbits \mathfrak{M} of elements of \mathcal{M} . Notice that all the faces corresponding to the elements of \mathfrak{D} now satisfy (i) and (ii) in Condition 1.

We remark that since the closure generally adds more elements to $\mathcal{D} \cup \{\mathbf{E}\}$, it can also happen that even though another element \mathbf{E}' is in a different orbit of \mathcal{M} , $\text{cl}_{\text{FD}}(\mathcal{D} \cup \{\mathbf{E}'\})$ is related to $\text{cl}_{\text{FD}}(\mathcal{D} \cup \{\mathbf{E}\})$ by an element of $G_{\mathcal{D}}$, in which case the two corresponding faces are considered equivalent. This equivalence is checked by Algorithm 3, allowing us to extract an even smaller collection of representative faces \mathfrak{D} , and to partition the elements of \mathcal{M} that have not been added to $\bar{\mathcal{U}}$ into even larger sets (the elements of \mathfrak{M}), each set being the union of elements of \mathfrak{M} .

To summarize, we have thus far used the closure operator cl_{FD} and the symmetries of the problem to identify a representative for each possible orbit of D-faces on the boundary of \mathcal{F} that contain at least one element of \mathcal{M} in their respective down-sets. The set of such representatives is \mathfrak{D} . We have further organized the elements of \mathcal{M} into two sets: those generating new faces which we can ignore are in $\bar{\mathcal{U}}$, and those in \mathfrak{M} where each component of this partition is associated with one element of \mathfrak{D} . We will now describe how to use this data to generate new triplets (see Algorithm 4) by specifying an excluded region for each face corresponding to a down-set in \mathfrak{D} .

First, we reorder the elements of \mathfrak{D} according to the function g in Function 2. It is clear that if we specify the excluded region for each face in \mathfrak{D} to be just $\bar{\mathcal{U}}$, we are guaranteed to not miss any $\vec{\mathcal{F}} \in \mathcal{F}$ which is not in $\hat{\mathcal{F}}$ because such D-ERs do not include any element of $\bar{\mathcal{U}}$ in their respective down-sets; however, this would be very inefficient. Instead, only the first triplet will have the excluded region be $\bar{\mathcal{U}}$, and this triplet will be the input into the next iteration of the main subroutine. As for the second triplet, we can now include in its excluded region not only $\bar{\mathcal{U}}$, but also all the elements in the first component of \mathfrak{M} since any D-ER associated to a down-set containing such an element will be obtained when we input the first triplet into the main subroutine during a later iteration. In a similar manner, we can for the third triplet include in its excluded region the union of $\bar{\mathcal{U}}$ and the first two components of \mathfrak{M} , and so on. Thus, we are able to enlarge the excluded region beyond $\bar{\mathcal{U}}$ for all except the first triplet, thereby increasing the efficiency of the algorithm without missing any D-ER $\vec{\mathcal{F}} \in \mathcal{F}$ not belonging in $\hat{\mathcal{F}}$. We stress that the specific choice of function g only affects the efficiency of the algorithm, and not its completeness. In other words, our proof that the algorithm is complete is independent of this function.

We then use Algorithm 5 to enforce (iii) in Condition 1 and to enlarge the excluded region of each new triplet even more by simply adding any element whose inclusion would, under the closure operator, cause the further addition of an element in the excluded region. It is clear that this does not affect completeness. We can efficiently implement this enlargement by again organizing these elements into orbits under the action of the stabilizer

group of the triplet, such that (iii) in Condition 1 remains satisfied.

The final step in the main subroutine is to check (iv) in Condition 1. By following the procedure given in the description of line 7 in Algorithm 2, we ensure that we do not miss any D-ERs associated to triplets that fail this condition. This completes the proof. \square

Of course, in the case where the function f in Function 1 is chosen such that at the end of the computation $\check{\mathcal{T}}$ is non-empty, one would then employ other, possibly more efficient at that stage, methods to extract the D-ERs. Furthermore, notice that for some D-ERs, the output might contain multiple representatives of the same G -orbit. We will comment on these issues in the next paragraph.

Post-processing: When the set-up is sufficiently simple such that the algorithm is stopped only when there are no more triplets to be processed, all the desired D-ERs will be contained in the set \mathfrak{R} . However, it should be noticed that in general \mathfrak{R} might contain more than one representative for each G -orbit, and to get exactly one representative per G -orbit one should still check equivalence of the various D-ERs under the action of G .

For harder problems, it might instead be convenient to stop the computation earlier, when some of the triplets in $\check{\mathcal{T}}$ correspond to higher-dimensional faces. Typically, this is the case when for each triplet that remains to be processed, the sub-poset induced by $\mathcal{E} \setminus (\mathcal{D} \cup \mathcal{U})$ is “approximately an antichain”, or more precisely, when the down-set of each maximal element of this sub-poset is a small subset of the sub-poset. In this situation, it is typically more efficient to use a standard conversion algorithm to extract all extreme rays of a face, and then check which extreme rays are D-ERs.

Nevertheless, we stress that even when using standard conversion algorithms, it might still be possible to speed up this computation significantly using the set \mathcal{U} that specifies the excluded region.⁴⁰ To see this, consider a triplet $(\mathcal{D}, \mathcal{U}, G_{\mathcal{D}})$ for a face \mathcal{F} , and suppose that \mathcal{U} is a “large subset” of \mathcal{E} , i.e., that $|\mathcal{U}|/|\mathcal{E}| \sim 1$. On the subspace spanned by \mathcal{F} , which is determined by \mathcal{D} , \mathcal{F} is a pointed cone carved out by the inequalities corresponding to the elements of $\mathcal{E} \setminus \mathcal{D}$. On this subspace, consider the larger cone $\check{\mathcal{F}}$ carved out by the inequalities given by $\mathcal{E} \setminus (\mathcal{D} \cup \mathcal{U})$. Notice that since the triplet we are considering is in the output of the algorithm, it satisfies in particular (iv) in Condition 1, implying that this cone is pointed. While the ERs of $\check{\mathcal{F}}$ are in general different from those of \mathcal{F} , notice that any ER of \mathcal{F} which does not saturate any inequality from \mathcal{U} (i.e., that is not in the excluded region $\hat{\mathcal{F}}$) is also an ER of $\check{\mathcal{F}}$. Since $\check{\mathcal{F}}$ is specified by a much smaller set of inequalities compared to \mathcal{F} , finding its ERs using standard conversion algorithm can be much simpler.

Suppose now that this is the case, that we have performed this computation and have found all the ERs of \mathcal{F} outside of $\hat{\mathcal{F}}$. We now need to extract the subset of D-ERs. Typically, one finds the ERs in a basis for the subspace of \mathcal{F} rather than that for the full space. Since the poset \mathcal{E} is defined in the full space where \mathcal{C} lives, in order to check if an ER is a D-ER, one should first perform a change of basis to recover the expression of the ER in the full space. However, if the number of both ERs and dimensions is large, this is not the most convenient

⁴⁰ This trick was indeed crucial for the derivation of the results presented in §5.

strategy. Instead, one can pre-compute a set of necessary conditions that must be satisfied by the set of inequalities which are saturated by an ER for it to be a D-ER, and then check these conditions “locally” on the lower-dimensional subspace spanned by \mathcal{F} . These conditions essentially stem from the fact that if an inequality corresponding to an element $E_i \in \mathcal{E}$ is saturated, all inequalities corresponding to the elements $E_j \in \mathcal{E}$ with $E_j \prec E_i$ also have to be saturated. In the full space, this last requirement is obviously also sufficient (since it is the definition of a down-set), but it may not be verifiable in the lower-dimensional subspace. The reason is essentially the fact that in general several inequalities which are distinct in the full space are indistinguishable in the lower-dimensional space. Nonetheless, one can derive local necessary conditions by restricting this requirement to the set of dimensionally reduced inequalities. If \mathcal{E} is far from being an antichain, which as discussed above is the regime of utility of this algorithm, one can expect that in most situations the vast majority of the ERs of \mathcal{F} will already fail these simpler necessary conditions and can therefore be more efficiently discarded as candidate D-ERs. It then suffices to recover the full expression of a much smaller collection of ERs in the space of \mathcal{C} to finally verify which ERs are D-ERs using the complete poset structure.

3.4 A few possible variations

We now describe a few possible variations of the algorithm. We will use some of them to derive the results presented in §4 and §5.

Checking symmetries: Notice that in Algorithm 1, the main subroutine is iterated on *all* outputs of previous iterations until the criterion to stop the computation is met. Some triplets that are generated during the computation however might belong to the same G -orbit. One possible variation of the algorithm would check this equivalence and select a representative for each orbit, deleting other triplets so that they will not be processed again. It is obvious that this simplification still guaranties the completeness of the result, as at least one representative for each orbit of D-ER which is not in the excluded region will be included in at least one of the faces of the final output. The convenience of implementing this variation depends on the specific problem, and in particular on the “size” of the orbits and on how efficiently one can check the equivalence of various faces.

Simplicial cones: Another simple variations considers the possibility that some of the faces generated during the computation might be *simplicial* cones. This is trivial to verify, since it only requires to check if the number of inequalities equals the dimension of the face. If a simplicial face is found, then instead of iterating the main subroutine for this face it is much more efficient to simply extract the D-ERs directly from the set of inequalities that specify the face.

Focusing on a lower-dimensional face: In some situations one might be interested in finding only the D-ERs that belong to a lower-dimensional face \mathcal{F} of the cone. For example, this is the case for the SAC, where as a result of Theorem 1, we can focus on the face \mathcal{F}_* that we mentioned in the Introduction. In these situations, it would seem natural to first simplify the problem via a dimensional reduction to the subspace spanned by \mathcal{F} ,

and then apply the algorithm to the resulting set-up. However, as we discussed above when we commented on the post-processing of the ERs, the full structure of the poset is not “completely visible” in a lower-dimensional subspace. One practical alternative is to instead initialize the algorithm setting $\mathcal{D}^{(0)} = \mathcal{V}(\mathcal{F})$ instead of $\mathcal{D}^{(0)} = \emptyset$.⁴¹

Using different closure operators: In the main subroutine described in Algorithm 2, we have used the closure operator cl_{FD} . While this closure can be computed efficiently using a linear program [28], for a large number of inequalities in a space with a large number of dimensions, this can still be a heavy computation. One alternative is to use cl_{LD} instead (see §3.2), which can be computed much more easily. This is in fact what we used in the computations presented in §4 and §5. Since this is a closure operator, the proof of completeness given in Theorem 2 remains essentially unchanged. Each triplet now corresponds not necessarily to a face, but to a linear subspace such that \mathcal{D} is a down-set. We will call such a linear subspace a D-subspace. When there is a face \mathcal{F} that spans this subspace, then \mathcal{F} is a D-face and corresponds to one of the usual triplets. More generally, it can instead happen that the subspace only contains a proper lower-dimensional subspace spanned by a face, which is then not guaranteed to be a D-face. In practical terms however, the only difference in the algorithm is in the main subroutine, since other subroutines do not use any closure operator. Further, in the main subroutine, the only difference is that when we obtain a triplet corresponding to a 1-dimensional subspace, this subspace is now not guaranteed to be spanned by an ER, and we need to verify that it contains a ray that satisfies all the inequalities. Finally, when the algorithm is used not to find all D-ERs directly, but rather only to extract a simpler set of faces that includes all D-ERs, if we replace cl_{FD} with cl_{LD} , we are now extracting a set of D-subspaces, although as we mentioned above they are not necessarily spanned by corresponding D-faces. The final result, however, is not affected by this difference, since the dimensional reduction of the remaining inequalities to this subspace will still specify a face of the cone, and even if this might not be a D-face, we will check during the post-processing which ERs we found are D-ERs.

4 A simple example: $N = 5$

Having explained our algorithm in §3 in full generality, we now return to the set-up described in §1 and §2 to exemplify the application of the algorithm to the SAC. Specifically, we will use it to compute the subset of $\mathcal{R}_{\text{KC}}^5$ of “genuine 5-party” ERs, i.e., those that are not lifts of element of $\mathcal{R}_{\text{KC}}^N$ for some $N < 5$. These ERs are well-known,⁴² and our goal here is simply to demonstrate how our algorithm works in a particular example. In the next section, we will use the algorithm to compute the much more involved $\mathcal{R}_{\text{KC}}^6$ (with the main goal of finding $\mathcal{R}_{\text{SSA}}^6$), and there we will only present the result.

To initialize the algorithm, we will use Theorem 1 of §2.1 to implement a variation of the algorithm described above and focus on the lower-dimensional KC-face \mathcal{F}_* , which

⁴¹ Here we are assuming that \mathcal{F} is a D-face. If it is not, then one should simply set $\mathcal{D}^{(0)} = \text{cl}_{\text{FD}}(\mathcal{V}(\mathcal{F}))$.

⁴² It was shown in [6] that $\mathcal{R}_{\text{KC}}^5 = \mathcal{R}_{\text{SSA}}^5$, and $\mathcal{R}_{\text{SSA}}^5$ was computed in [5].

contains the KC-ERs not realized by Bell pairs. This means that to specify the initial triplet $\mathfrak{T}^{(0)}$, we can set

$$\mathcal{D}^{(0)} = \mathcal{V}(\mathcal{F}_*) = \{I(\ell : \ell'), \text{ for all } \ell, \ell' \in \llbracket 5 \rrbracket\}. \quad (4.1)$$

Furthermore, since we are only focusing on genuine 5-party KC-ERs, we can use the constraints described in §2.2 and specify the excluded region $\widehat{\mathcal{C}}$ of the cone to be

$$\mathcal{U}^{(0)} = \{I(\underline{\mathcal{J}} : \underline{\mathcal{K}}), 5 \leq |\underline{\mathcal{J}}| + |\underline{\mathcal{K}}| \leq 6\}. \quad (4.2)$$

The cardinalities of these sets are $|\mathcal{D}^{(0)}| = 15$ and $|\mathcal{U}^{(0)}| = 121$. Lastly, the symmetry group G is a subgroup of $\text{Sym}(270)$ (since $|\mathcal{E}| = 301$, but the 31 top elements of the MI-poset correspond to redundant inequalities) isomorphic to $\text{Sym}(6)$, which is the group of all permutations for the six parties in $\llbracket 5 \rrbracket$. Hence, we set $G^{(0)} = G$.

Moreover, we will use two of the variations mentioned in §3.4 when implementing the basic algorithm presented in §3.3. The first variation is that we will use the closure operator cl_{LD} instead of cl_{FD} in the main subroutine. Each triplet will then correspond to a KC-subspace⁴³ rather than a KC-face. The reason for this choice is that computing cl_{LD} is typically much faster than computing cl_{FD} , and empirical observation suggests that most instances of KC-subspaces are in fact spanned by KC-faces. Thus, using cl_{FD} instead of cl_{LD} would not give a significant advantage, while dramatically slowing down the computation. We will continue to use the same strategy in the next section.

The second variation, which we only use here for the purpose of illustration, consists of checking if any of the faces generated during the computation is a simplicial cone. If so, we can simply extract the KC-ERs directly without having to continue iterating through the main subroutine of our algorithm. A schematic description of the various steps of the computation is given in Figure 3, and we now describe a few of these steps in detail.

With these two additional variations in mind, and having specified the initial triplet $\mathfrak{T}^{(0)}$, we need to choose the criteria to stop the computation and to generate the triplets with the main subroutine. For $N = 5$, the computation is sufficiently simple that we stop only after processing all the triplets, therefore finding all the desired ERs without having to rely on other algorithms. This corresponds to setting the function f in Function 1 to return TRUE only if the dimension of a KC-subspace is at most one. Meanwhile, a convenient choice for Function 2 is the dimension of the KC-subspaces corresponding to the newly generated down-sets. In this way, the dimension of these subspaces will be increasing along the sequence, and subspaces with greater dimension will be associated to larger excluded regions.

The first iteration of the main subroutine on the triplet $(\mathcal{D}^{(0)}, \mathcal{U}^{(0)}, G^{(0)})$ begins by computing the maximal elements $\mathcal{M}^{(0)}$ of $\mathcal{E} \setminus (\mathcal{D}^{(0)} \cup \mathcal{U}^{(0)})$ and organizing them into $G^{(0)}$ -

⁴³ As the reader might guess, a KC-subspace is precisely the D-subspace defined in §3 when the poset is the MI-poset. Similarly, KC-faces and KC-ERs are respectively the D-faces and D-ERs defined above when the poset is the MI-poset.

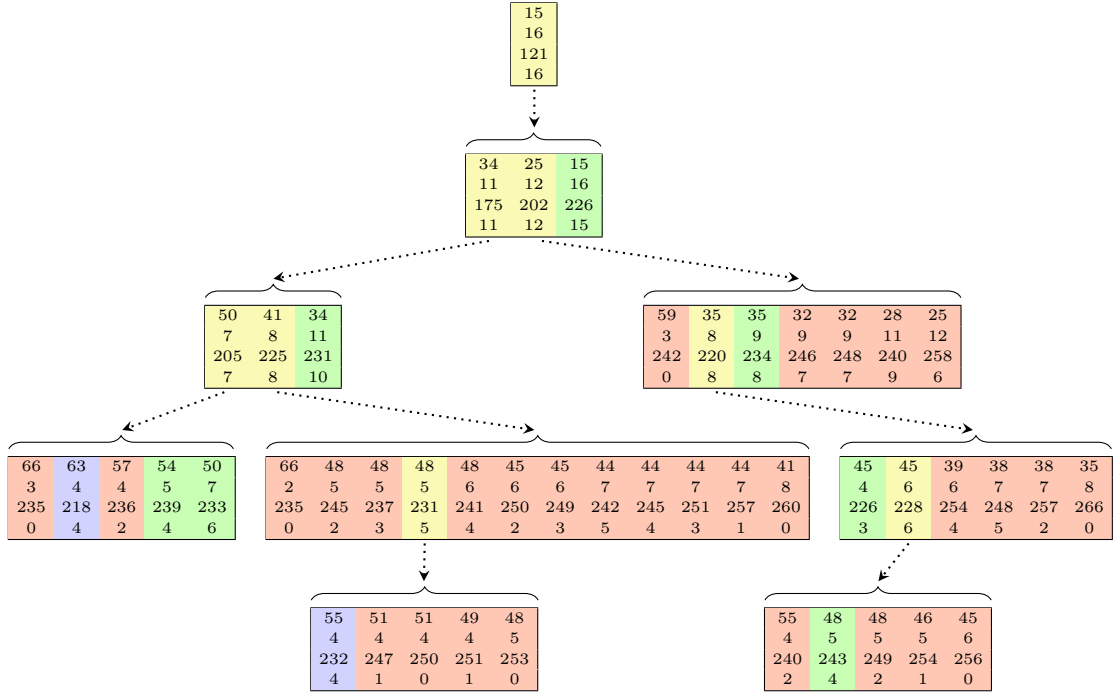


Figure 3: A schematic illustration of the various steps of the computation of $\mathcal{R}_{\text{KC}}^5$, where each box corresponds to one iteration of the main subroutine. In each box, each column corresponds to one of the triplets in \mathcal{T} after the completion of line 5 in Algorithm 2. For each triplet \mathcal{T} , the four rows from top to bottom are as follows: the cardinality of \mathcal{D} ; the dimension of the KC-subspace specified by \mathcal{D} ; the cardinality of \mathcal{U} ; and the rank of $\mathcal{E} \setminus (\mathcal{D} \cup \mathcal{U})|_{\mathcal{D}}$, where the subscript \mathcal{D} indicates we are considering the dimensional reduction of the inequalities to the KC-subspace specified by \mathcal{D} , since we are working with KC-subspaces rather than D-faces. The various triplets are further distinguished by color depending on the following: whether they satisfy Condition 1 but the corresponding faces are not simplicial (yellow); whether they satisfy Condition 1 and the corresponding faces are simplicial (blue); whether (3.17) holds and they correspond to a D-ER (green); or whether (3.18) is satisfied and they can be discarded (red). For each yellow triplet, the arrow indicates which box presents the data of the corresponding new iteration of the main subroutine. The box at the top shows the data for the initial triplet $\mathcal{T}^{(0)}$, and the box immediately below it shows the data for the triplets $\mathcal{T}^{(0,1)}$, $\mathcal{T}^{(0,2)}$ and $\mathcal{T}^{(0,3)}$, which are described in detail in the main text.

orbits. We obtain two orbits, which have the form

$$\begin{aligned} \mathcal{M}_1 &= \{l(\underline{j} : \underline{\mathcal{K}}) \in \mathcal{E}, |\underline{j}| = 2 \quad |\underline{\mathcal{K}}| = 2\} \\ \mathcal{M}_2 &= \{l(\underline{j} : \underline{\mathcal{K}}) \in \mathcal{E}, |\underline{j}| = 3 \quad |\underline{\mathcal{K}}| = 1\}. \end{aligned} \quad (4.3)$$

Choosing the representative $l(12 : 34)$ from the first orbit we get

$$\begin{aligned} \mathcal{D}_1 &= \text{cl}_{\text{LD}} \left[\mathcal{D}^{(0)} \cup \{l(12 : 34)\} \right] \\ &= \{l(12 : 34), l(13 : 24), l(14 : 23), l(123 : 4), l(124 : 3), l(134 : 2), l(234 : 1)\}_{\downarrow} \cup \mathcal{D}^{(0)}, \end{aligned} \quad (4.4)$$

where $\{\dots\}_{\downarrow}$ denotes the down-set generated by the elements in the argument. Hence

$|\mathcal{D}_1| = 34$. Choosing instead the representative $l(123 : 4)$ from the second orbit gives

$$\begin{aligned} \mathcal{D}_2 &= \text{cl}_{\text{LD}} \left[\mathcal{D}^{(0)} \cup \{l(123 : 4)\} \right] \\ &= \{l(123 : 4), l(14 : 2), l(14 : 3), l(24 : 1), l(24 : 3), l(34 : 1), l(34 : 2)\} \downarrow \cup \mathcal{D}^{(0)}, \end{aligned} \quad (4.5)$$

so $|\mathcal{D}_2| = 25$. Since neither \mathcal{D}_1 nor \mathcal{D}_2 contain any element of $\mathcal{U}^{(0)}$, they are not in the excluded region, and we have $\bar{\mathcal{U}} = \mathcal{U}^{(0)}$ (see line 1 in Algorithm 2). Furthermore, it is immediate to verify that these down-sets correspond to faces of dimension greater than one, and since they are clearly not related by a permutation of the parties, they are also the elements of $\check{\mathfrak{D}}$, the output of Algorithm 3. We can then apply to them (and the sets \mathcal{M}_1 and \mathcal{M}_2 in $\check{\mathfrak{M}}$) Algorithm 4 to generate two new inequivalent triplets $(\mathcal{D}^{(0,1)}, \mathcal{U}^{(0,1)}, G^{(0,1)})$ and $(\mathcal{D}^{(0,2)}, \mathcal{U}^{(0,2)}, G^{(0,2)})$, with $\mathcal{D}^{(0,1)} = \mathcal{D}_1$ and $\mathcal{D}^{(0,2)} = \mathcal{D}_2$, and $\mathcal{U}^{(0,1)} = \mathcal{U}^{(0)}$ and $\mathcal{U}^{(0,2)} = \mathcal{U}^{(0)} \cup \mathcal{M}_1$. Furthermore, the groups $G^{(0,1)}$ and $G^{(0,2)}$ are the following subgroups of $\text{Sym}(270)$:

$$\begin{aligned} G^{(0,1)} &\simeq \text{Sym}(4)_{1234} \times \text{Sym}(2)_{50} \\ G^{(0,2)} &\simeq \text{Sym}(3)_{123} \times \text{Sym}(2)_{50}, \end{aligned} \quad (4.6)$$

where the lower indices indicate the specific parties which are permuted by the various factors. Notice that as mentioned above, the ordering is chosen such that the dimension of the corresponding KC-subspace is increasing from \mathcal{D}_1 to \mathcal{D}_2 .

These two triplets are the input of Algorithm 5, which we can now use to “extend” the excluded region. There are 146 elements in $\mathcal{E} \setminus (\mathcal{D}^{(0,1)} \cup \mathcal{U}^{(0,1)})$, which can be organized into 11 different $G^{(0,1)}$ -orbits with the following representatives:

$$\begin{aligned} &l(1 : 50), l(15 : 0), l(1 : 250), l(15 : 20), l(12 : 50), l(125 : 0), \\ &l(1 : 25), l(12 : 5), l(12 : 35), l(123 : 5), l(1 : 235). \end{aligned} \quad (4.7)$$

Similarly, in $\mathcal{E} \setminus (\mathcal{D}^{(0,2)} \cup \mathcal{U}^{(0,2)})$ there are 110 elements, and they can be organized into 21 different $G^{(0,2)}$ -orbits with the following representatives:

$$\begin{aligned} &l(4 : 50), l(45 : 0), l(150 : 4), l(145 : 0), l(1 : 250), \\ &l(1 : 234), l(1 : 450), l(1 : 45), l(15 : 4), l(1 : 50), l(15 : 0), l(14 : 5), l(1 : 245), \\ &l(1 : 25), l(125 : 4), l(12 : 5), l(125 : 0), l(124 : 5), l(1 : 235), l(1 : 23), l(123 : 5). \end{aligned} \quad (4.8)$$

One can verify that for any MI instance l in the first row of (4.7), or any MI instance l' in the first row of (4.8), we have

$$\begin{aligned} \text{cl}_{\text{LD}} \left[\mathcal{D}^{(0,1)} \cup \{l\} \right] \cap \mathcal{U}^{(0,1)} &\neq \emptyset \\ \text{cl}_{\text{LD}} \left[\mathcal{D}^{(0,2)} \cup \{l'\} \right] \cap \mathcal{U}^{(0,2)} &\neq \emptyset. \end{aligned} \quad (4.9)$$

Therefore, Algorithm 5 respectively adds to $\mathcal{U}^{(0,1)}$ and $\mathcal{U}^{(0,2)}$ all the elements belonging to the orbits of the MI instances in the first rows of (4.7) and (4.8). The resulting triplets (with $\mathcal{D}^{(0,1)}$ and $\mathcal{D}^{(0,2)}$, and therefore $G^{(0,1)}$ and $G^{(0,2)}$, unchanged) automatically satisfy (iii) in Condition 1 by construction.

The next step of the main subroutine takes into account the possibility of relevant down-sets that include $\mathcal{D}^{(0)}$ but no element of $\mathcal{M}^{(0)}$ (see line 5 in Algorithm 2), thereby generating a third triplet $(\mathcal{D}^{(0,3)}, \mathcal{U}^{(0,3)}, G^{(0,3)})$, where

$$\begin{aligned}\mathcal{D}^{(0,3)} &= \mathcal{D}^{(0)} \\ \mathcal{U}^{(0,3)} &= \mathcal{U}^{(0)} \cup \mathcal{M}^{(0)} \\ G^{(0,3)} &= G^{(0)}.\end{aligned}\tag{4.10}$$

Having constructed these triplets, we now need to verify that they satisfy (iv) in Condition 1. For the first two triplets, we leave it as an exercise for the reader to check that this is indeed the case. The last triplet, on the other hand, fails this condition, and we can immediately derive from it a “candidate” D-ER from the simultaneous saturation of all inequalities corresponding to the elements of $\mathcal{E} \setminus \mathcal{U}^{(0,3)}$. This is a 1-dimensional KC-subspace generated by the entropy vector

$$\vec{S} = \{1, 1, 1, 1, 1; 2, 2, 2, 2, 2, 2, 2, 2, 2, 2; 3, 3, 3, 3, 3, 3, 3, 3, 3; 2, 2, 2, 2, 2; 1\}.\tag{4.11}$$

Since \vec{S} satisfies all instances of SA, it follows that it is an element of $\mathcal{R}_{\text{KC}}^5$. A schematic summary of the further iterations of the main subroutine for the rest of the computation of $\mathcal{R}_{\text{KC}}^5$ is shown in Figure 3.

5 Results for $N = 6$

Having exemplified the workings of our algorithm for the $N = 5$ case, we now present the results of the algorithm applied to finding the KC-ERs of SAC_6 , primarily focusing on the ones that satisfy SSA.⁴⁴ The algorithm produced 220 orbits of genuine 6-party ERs in $\mathcal{R}_{\text{KC}}^6$, and upon checking SSA, we find that 12 of these in fact violate at least one instance of SSA (cf. §5.1).⁴⁵

A natural first step towards classifying the orbits of $\mathcal{R}_{\text{SSA}}^6$ is to determine which ERs violate some *holographic entropy inequality* (HEI). However, since the complete set of $N = 6$ HEIs is unknown, in principle this only specifies a subset of $\mathcal{R}_{\text{SSA}}^6$ which includes, but not necessarily coincides with, $\mathcal{R}_{\text{Hol}}^6$. Using all the hitherto found HEIs (of which there are currently 1,877, as detailed in [32]), we find that there are 52 orbits which violate at least one instance of these inequalities; these are discussed in §5.2.

The remaining 156 orbits are candidates for $\mathcal{R}_{\text{Hol}}^6$, and in order to classify them as such, it suffices to find a holographic graph model which realizes the given entropy vector. In §5.3, we summarize the result of this endeavor, presenting graphs for 150 ERs. This leaves only 6 unclassified orbits, which we dub “mystery” ERs, and we further comment on them in §5.4.

⁴⁴ Further details are presented in [24], in particular their adjacency relation, their characterization in terms of the β -sets of [31], and our procedure to obtain graph models that realize most of them.

⁴⁵ Unlike the $N \leq 5$ computations, we find that for $N = 6$ there in fact even exist 1-dimensional KC-subspaces which are not extreme rays of SAC_6 because they violate at least one instance of SA. An example of such a subspace is that generated by $\vec{s} = \{4, 2, 3, 2, 2, 3; 6, 7, 6, 6, 7, 5, 4, 4, 5, 5, 5, 6, 4, 5, 5; 7, 8, 8, 9, 9, 9, 8, 8, 9, 9, 7, 7, 8, 6, 7, 5, 7, 8, 8, 7; 9, 9, 8, 10, 7, 9, 9, 8, 6, 9, 9, 10, 8, 11, 10; 7, 6, 6, 7, 6, 8; 4\}$.

In Table 4, we present the entropy vectors of a representative instance from every orbit in $\mathcal{R}_{\text{SSA}}^6$ (this data can also be found in the supplementary materials), where we did not include the lifts of the elements of $\mathcal{R}_{\text{SSA}}^6$ for $N < 6$. Following the usual convention, the components of each vector are arranged by the cardinality of the subsystems \mathcal{J} (separated by semicolon for ease of identification), and within each group they are arranged in lexicographic order. For convenience, we also color-code each ER by its type: Warm colors (pink, red, orange, yellow) represent holographic ERs (those definitely in \mathcal{R}_{Hoi}), cold colors (blue, violet) represent ERs that violate at least one HEI (those definitely in $\mathcal{R}_{\text{SSA}} \setminus \mathcal{R}_{\text{Hoi}}$), and green represents the remaining mystery ERs. This color scheme is further subdivided as follows. Pink ERs are realized by star graphs, red ones by other simple⁴⁶ tree graphs, and orange and yellow ones by more complicated graphs. The orange ones were known previously [33], while the yellow ones are new, illustrating the power of our construction. Notice that since all ERs of the SAC which can be realized by graph models are simultaneously ERs of the HEC, the yellow ERs yield previously unknown ERs of the $N = 6$ HEC. Finally, among the ERs that violate some HEI, we distinguish the ones which violate MMI by blue and the ones which only violate some higher $N = 5, 6$ HEI by purple.

Labeling each orbit in $\mathcal{R}_{\text{SSA}}^6$ by an index $s \in [208]$, the coarse breakdown of holographic versus non-holographic ER orbits is given by the following three categories.

- The **52** “non-holographic” ERs that violate some HEI, and are therefore in $\mathcal{R}_{\text{SSA}} \setminus \mathcal{R}_{\text{Hoi}}$, are generated by the entropy vectors \vec{S}_s , with s in $\{71, 108, 118, 124, 126, 132, 133, 140, 141, 142, 143, 144, 148, 150, 153, 154, 158, 160, 162, 163, 164, 165, 166, 167, 173, 174, 175, 176, 177, 178, 179, 182, 183, 184, 185, 186, 187, 188, 191, 192, 193, 194, 197, 198, 199, 200, 201, 202, 203, 204, 205, 208\}$. We discuss these further in §5.2.
- The **150** ERs that can be realized by holographic graph models, and are therefore in \mathcal{R}_{Hoi} , are generated by the entropy vectors \vec{S}_s , with s in $\{1, 2, 3, 4, 5, 6, 7, 8, 9, 10, 11, 12, 13, 14, 15, 16, 17, 18, 19, 20, 21, 22, 23, 24, 25, 26, 27, 28, 29, 30, 31, 32, 33, 34, 35, 36, 37, 38, 39, 40, 41, 42, 43, 44, 45, 46, 47, 48, 49, 50, 51, 52, 53, 54, 55, 56, 57, 58, 59, 60, 61, 62, 63, 64, 65, 66, 67, 68, 69, 70, 72, 73, 74, 75, 76, 77, 78, 79, 80, 81, 82, 83, 84, 85, 86, 87, 88, 89, 90, 91, 92, 93, 94, 95, 96, 97, 98, 99, 100, 101, 102, 103, 104, 105, 106, 107, 109, 111, 112, 113, 114, 115, 116, 117, 119, 120, 121, 122, 123, 125, 127, 128, 129, 130, 131, 134, 135, 136, 137, 138, 139, 147, 149, 151, 152, 155, 156, 157, 159, 161, 169, 170, 171, 172, 189, 190, 195, 196, 206, 207\}$. We discuss these further in §5.3.
- Finally, the remaining **6** “mystery” ERs that do not violate any known HEI, but thus far do not have a holographic graph model construction, are generated by the entropy vectors \vec{S}_s , with s in $\{110, 145, 146, 168, 180, 181\}$. We remark on these in §5.4.

Before focusing on these categories separately in the subsections below, in Table 5 we present several further attributes of the ERs in $\mathcal{R}_{\text{SSA}}^6$. Maintaining the same color-coding as in Table 4, we list for each orbit:

⁴⁶ By *simple* tree graphs, we mean graphs which have no cycles and have one boundary vertex per party.

- The total number of individual HEIs which are violated by the given ER (“#Q< 0”), and the number of HEI orbits containing a violated instance (“#Qo< 0”). These are of course non-zero only for the non-holographic ERs, so for the holographic and mystery ones we leave the entry blank to avoid clutter. The largest number of violated instances is 46,095, whereas the largest number of HEI orbits containing violated instances is 1,449. In §5.2, we will provide further details by distinguishing the types of HEIs.

5.1 The approximation of SSA by KC is not exact

ER#	#Q _{SSA} <0	Svec
209	3	(2,2,2,3,3,3; 4,4,5,5,5,4,5,5,5,5,5,5,6,6,6; 6,7,5,7,7,5,7,8,8,8,7,7,7,8,6,8,8,8,8,5; 9,5,5,8,8,8,8,8,5,8,8,8,5,7; 6,6,6,5,5,5; 3)
210	3	(2,2,2,3,3,3; 4,4,5,5,5,4,5,5,5,5,5,6,6,6; 6,7,5,7,7,7,5,8,8,8,7,5,7,8,8,8,8,8,8,5; 9,5,5,8,8,8,8,8,8,7,8,8,8,7,7; 6,6,6,5,5,5; 3)
211	1	(2,2,2,3,3,3; 4,4,5,5,5,4,5,5,5,5,5,6,6,6; 6,7,5,7,7,7,5,8,8,8,7,7,5,8,8,8,8,8,8,5; 9,7,5,8,8,8,8,8,6,7,8,8,8,7,7; 6,6,6,5,5,5; 3)
212	1	(2,2,2,3,3,3; 4,4,5,5,5,4,5,5,5,5,5,6,6,6; 6,7,5,7,7,7,5,8,8,8,7,7,5,8,8,8,8,8,8,5; 9,7,5,8,8,8,8,8,8,7,8,8,8,7,7; 6,6,6,5,5,5; 3)
213	3	(2,2,2,3,3,3; 4,4,5,5,5,4,5,5,5,5,5,6,6,6; 6,7,5,7,7,7,5,8,8,8,7,7,7,8,8,8,8,8,8,5; 9,5,5,8,8,8,8,8,8,5,8,8,8,7,7; 6,6,6,5,5,5; 3)
214	1	(2,2,2,3,3,3; 4,4,5,5,5,4,5,5,5,5,5,6,6,6; 6,7,5,7,7,7,5,8,8,8,7,7,7,8,8,8,8,8,8,5; 9,5,7,8,8,8,8,8,8,7,8,8,8,7,7; 6,6,6,5,5,5; 3)
215	1	(2,2,2,3,3,3; 4,4,5,5,5,4,5,5,5,5,5,6,6,6; 6,7,5,7,7,7,5,8,8,8,7,7,7,8,8,8,8,8,8,5; 9,7,5,8,8,8,8,8,8,5,8,8,8,7,7; 6,6,6,5,5,5; 3)
216	1	(2,2,2,3,3,3; 4,4,5,5,5,4,5,5,5,5,5,6,6,6; 6,7,7,5,7,7,7,8,8,8,7,7,7,8,6,8,8,8,8,5; 9,9,5,8,8,8,8,8,8,7,8,8,8,5,7; 6,6,6,5,5,5; 3)
217	3	(2,2,2,3,3,3; 4,4,5,5,5,4,5,5,5,5,5,6,6,6; 6,7,7,7,7,5,7,8,8,8,7,7,5,8,8,8,8,8,8,5; 9,5,5,8,8,8,8,8,8,7,8,8,8,7,7; 6,6,6,5,5,5; 3)
218	1	(2,2,2,3,3,3; 4,4,5,5,5,4,5,5,5,5,5,6,6,6; 6,7,7,7,7,5,7,8,8,8,7,7,5,8,8,8,8,8,8,5; 9,7,5,8,8,8,8,8,8,7,8,8,8,7,7; 6,6,6,5,5,5; 3)
219	1	(2,2,2,3,3,3; 4,4,5,5,5,4,5,5,5,5,5,6,6,6; 6,7,7,7,7,5,8,8,8,7,7,7,8,8,8,8,8,8,5; 9,9,5,8,8,8,8,8,8,5,8,8,8,7,7; 6,6,6,5,5,5; 3)
220	1	(2,3,2,2,3,4; 5,4,4,5,6,5,5,6,7,4,5,6,5,6,7; 5,7,8,9,6,7,8,7,8,9,7,8,9,8,9,10,7,6,9,9; 5,8,9,10,9,8,9,6,9,9,10,9,8,8,9; 8,7,6,6,7,6; 4)

Table 6: The entropy vectors for a choice of representatives for all orbits of ERs in $\mathcal{R}_{\text{KC}}^6 \setminus \mathcal{R}_{\text{SSA}}^6$. The second column indicates how many instances of SSA are violated by each given ER.

As anticipated above, some ERs in $\mathcal{R}_{\text{KC}}^6$ violate SSA, which means that in contrast to the situation for smaller values of N studied in [6], for $N \geq 6$ there is in fact a gap between \mathcal{R}_{KC} and \mathcal{R}_{SSA} . This means that the approximation of SSA by KC is not exact even for extreme rays. In particular, there are 12 orbits of ERs in $\mathcal{R}_{\text{KC}}^6 \setminus \mathcal{R}_{\text{SSA}}^6$, and in Table 6, we list the entropy vector of a representative for each orbit (using the same conventions as in Table 4). The table also shows the number of SSA instances which are violated by the given ER. Notice that there are very few instances that are violated: In four cases there are three, and in the remaining cases there is only a single one. While these ERs are not particularly interesting for any application, a more careful exploration of the combinatorial structure of their corresponding down-sets in the MI-poset might be useful to refine KC to a stronger condition that better approximates SSA and possibly improves the efficiency of the algorithm.

5.2 Extreme rays that violate holographic entropy inequalities

As we mentioned above, 52 of the 208 orbits of ERs in $\mathcal{R}_{\text{SSA}}^6$ violate some known HEI, and it is natural to further categorize these inequalities into three families: *monogamy of mutual information* (MMI) [34] (including its lifts), $N = 5$ HEIs [8, 23], and $N = 6$ HEIs [32] (the latter list is incomplete, so for this case the number of violations is merely a lower bound). Regarding the instances of MMI, up to permutations and purifications there are only three distinct possibilities for the cardinalities of the arguments of the *tripartite information*⁴⁷:

⁴⁷ The tripartite information is defined as $I_3(\mathcal{J} : \mathcal{J} : \mathcal{K}) = S_{\mathcal{J}} + S_{\mathcal{J}} + S_{\mathcal{K}} - S_{\mathcal{J}\mathcal{J}} - S_{\mathcal{J}\mathcal{K}} - S_{\mathcal{J}\mathcal{K}} + S_{\mathcal{J}\mathcal{J}\mathcal{K}}$, and MMI is the statement that $I_3(\mathcal{J} : \mathcal{J} : \mathcal{K}) \leq 0$.

ER#	# MMI<0	# N5<0	# N6<0	# Q<0	# MMIo<0	# N5o<0	# N6o<0	# Qo<0
71	1			1	1			1
108	1		151	152	1		30	31
118	1	8	5291	5300	1	5	846	852
124	1		364	365	1		97	98
126	1		504	505	1		114	115
132	1		1578	1579	1		264	265
133	1		929	930	1		191	192
140	2		1904	1906	1		178	179
141		1	20	21		1	5	6
142		1	236	237		1	62	63
143		1	105	106		1	30	31
144		1	40	41		1	3	4
148	1	7	4394	4402	1	5	1246	1252
150	1		791	792	1		218	219
153	1		449	450	1		143	144
154	1		1216	1217	1		317	318
158	1	7	2380	2388	1	5	889	895
160	1		820	821	1		196	197
162	1		151	152	1		73	74
163	1		759	760	1		228	229
164	1		277	278	1		88	89
165		1	164	165		1	48	49
166		1	230	231		1	108	109
167	4		11 868	11 872	1		306	307
173	1		1516	1517	1		332	333
174	1		1485	1486	1		295	296
175	1	7	2849	2857	1	5	868	874
176	1	7	2747	2755	1	5	871	877
177	2		5454	5456	1		518	519
178	2		1373	1375	1		191	192
179	2	14	10 178	10 194	1	5	1130	1136
182		1	238	239		1	111	112
183	1		1741	1742	1		280	281
184	1		1575	1576	1		297	298
185	2		1405	1407	1		294	295
186	2		603	605	1		132	133
187	7		46 088	46 095	1		296	297
188	1		1154	1155	1		267	268
191	2		2727	2729	1		346	347
192	3		4194	4197	1		336	337
193	1		888	889	1		262	263
194	1		494	495	1		143	144
197	1	17	9283	9301	1	5	1443	1449
198	1		1370	1371	1		370	371
199	2	14	5708	5724	1	4	846	851
200	1		1557	1558	1		349	350
201	1		762	763	1		282	283
202	3		8670	8673	1		469	470
203	1		1244	1245	1		353	354
204	2	12	6375	6389	1	4	996	1001
205	4	28	24 446	24 478	1	4	1046	1051
208	1		1184	1185	1		287	288

Table 7: A summary of the orbits of ERs in \mathcal{P}_{SSA}^6 that violate at least one known HEI. The rows list the ER label s , with the same color-coding as in Table 4. The columns specify the total number of HEIs which are violated by the given ER, broken down into MMI, $N = 5$ HEIs, $N = 6$ HEIs (normal color) and the total number of HEI instances (lighter color), as well as the corresponding number of orbits admitting a violated instance (darker color) and the total (lighter).

(1:1:1), (1:1:2), and (1:2:2). As it turns out, only the last type can be violated.

In Table 7, we list the number of violations by family (MMI / $N = 5$ / $N = 6$), both for individual instances and for their orbits. For convenience, we also present the total number of violations (which has already appeared in Table 5). There are 45 MMI-violating ER orbits, out of which only #71 does not violate any HEI for larger N . All the remaining 51 orbits instead violate some $N = 6$ HEI, and 17 of them also violate some $N = 5$ HEI. On the other hand, not a single orbit violates only HEI for $N = 6$, and only seven orbits do not violate any instance of MMI. This seems to suggest that at a given N , it is sufficient to know the HEI for some values of $N' \leq N$ to determine which elements of \mathcal{R}_{SSA} are in \mathcal{R}_{Hol} , and it would be interesting to explore this behavior more deeply.

Although we do not have good control over \mathcal{R}_{QM} beyond the nesting indicated by (1.9), we have previously constructed hypergraph realizations for some of these ERs. In particular, #118 is given by (a permutation of) the hypergraph in [16, Fig.1] and #71 is given by the hypergraph in [7, Fig.1]. We stress however that we have not attempted here to realize other ERs by hypergraphs, and it is entirely possible that they are in fact all realizable. We have checked the *hypergraph inequality* proven in [35], as well all instances of Ingleton inequality [36] (the main inequality characterizing the entropies of stabilizer states for four parties [15]), and found no violation.

5.3 Extreme rays realizable by holographic graph models

We now turn to the largest category, the 150 orbits of ERs which we explicitly realize by holographic graph models and therefore lie in \mathcal{R}_{Hol} .⁴⁸ Out of these orbits, 125 were already known to be holographic (although we found a simpler graph realization for 81 of them), while the remaining 25 are new. We present these results in Table 8, categorized by the same color-coding scheme as in the previous tables. For the former set, we indicate the corresponding label from [33]. We present two equivalent graphs for each ER: a simple version with one boundary vertex per party (these graphs therefore contain cycles for all but the 44 graphs corresponding to simple trees), and a “tree-ified” version where the boundary vertices are “fine-grained” so as to remove all cycles which include boundary vertices. In agreement with the strongest form of the conjecture in [1], most⁴⁹ of these graphs are tree graphs, though they may not be simple tree graphs. However, this means that they would represent simple tree graphs in a system with $N' > N$ parties (for some appropriate N'). In fact, for such N' , one can immediately verify that upon fine-graining, all these graphs realize ERs of $\text{SAC}_{N'}$. To quantify the necessary amount of fine-graining (or equivalently, the number of individual “splits” of boundary vertices), we indicate the graph complexity in the last column of Table 8. In particular, we list three attributes, denoted as $\{s,v,e\}$, which respectively specify the number of splits, the number of bulk vertices, and the total number of edges in the graph. Notice that many of the tree-ified graph models

⁴⁸ We relegate further discussion of graph construction, properties, and relations to [24]. Here, we only briefly summarize the results.

⁴⁹ For two ERs (#111 and #207), their corresponding graphs still each contains a “bulk cycle”, and it would be interesting to see if we can alternatively realize them by tree graphs. We leave this for future exploration.

ER	HEr	simple graph	graph	(s,v,e)
1	127			(0, 1, 7)
2	222			(0, 1, 7)
3	258			(0, 1, 7)
4	152			(0, 1, 7)
5	229			(0, 1, 7)
6	369			(0, 1, 7)
7	396			(0, 1, 7)
8	265			(0, 1, 7)
9	224			(0, 1, 7)
10	398			(0, 1, 7)
11	230			(0, 1, 7)
12	271			(0, 1, 7)
13	259			(0, 1, 7)
14	128			(0, 1, 7)
15	99			(0, 2, 8)
16	221			(0, 2, 8)
17	286			(0, 2, 8)
18	246			(0, 2, 8)
19	145			(0, 2, 8)
20	257			(0, 2, 8)
21	301			(0, 2, 8)
22	227			(0, 2, 8)
23	367			(0, 2, 8)
24	262			(0, 2, 8)
25	393			(0, 2, 8)
26	366			(0, 2, 8)
27	387			(0, 2, 8)
28	264			(0, 2, 8)
29	397			(0, 2, 8)
30	376			(0, 2, 8)
31	395			(0, 2, 8)
32	223			(0, 2, 8)
33	342			(0, 2, 8)
34	155			(0, 2, 8)
35	328			(0, 2, 8)
36	225			(0, 2, 8)
37	249			(0, 2, 8)
38	380			(0, 2, 8)
39	209			(0, 2, 8)
40	29			(0, 2, 8)
41	231			(0, 2, 8)
42	134			(0, 2, 8)
43	333			(0, 3, 9)
44	153			(0, 3, 9)
45	97			(1, 3, 10)
46	205			(1, 3, 10)
47	203			(1, 3, 10)
48	144			(1, 3, 10)
49	245			(1, 3, 10)
50	226			(1, 3, 10)
51	254			(1, 3, 10)
52	256			(1, 3, 10)
53	299			(1, 3, 10)
54	300			(1, 3, 10)
55	391			(1, 3, 10)
56	362			(1, 3, 10)
57				(1, 3, 10)
58	369			(1, 3, 10)
59	364			(1, 3, 10)
60	358			(1, 3, 10)
61	263			(1, 3, 10)
62	365			(1, 3, 10)
63	392			(1, 3, 10)
64	374			(1, 3, 10)
65	375			(1, 3, 10)
66	2922			(1, 3, 10)
67	286			(1, 3, 10)
68	337			(1, 3, 10)
69	341			(1, 3, 10)
70	371			(1, 3, 10)
72	281			(2, 3, 11)
73	282			(3, 4, 13)
74	253			(3, 3, 12)
75	255			(2, 4, 12)
76	297			(3, 4, 13)
77	296			(2, 3, 11)
78	293			(3, 2, 11)
79	298			(3, 2, 11)
80	356			(3, 2, 11)
81	361			(3, 4, 13)
82	359			(2, 3, 11)
83	353			(3, 4, 13)
84	42			(3, 4, 13)
85	357			(3, 3, 12)
86	363			(3, 4, 13)
87	2910			(3, 3, 12)
88				(2, 4, 12)
89				(3, 4, 13)
90				(2, 3, 11)
91				(3, 4, 13)
92	154			(1, 3, 10)
93	239			(1, 3, 10)
94	238			(1, 3, 10)
95	311			(1, 3, 10)
96	378			(1, 3, 10)
97	326			(1, 3, 10)
98	282			(2, 3, 11)
99	285			(3, 2, 12)
100	284			(3, 4, 13)
101	335			(2, 3, 11)
102	336			(3, 4, 13)
103	340			(2, 3, 11)
104	339			(3, 4, 13)
105	289			(2, 4, 12)
106	332			(2, 4, 12)
107	41			(6, 5, 17)
108	292			(3, 3, 12)
111	294			(2, 4, 13)
112	291			(3, 3, 12)
113				(4, 4, 14)
114				(6, 5, 17)
115				(4, 5, 15)
116				(5, 5, 16)
117	310			(2, 4, 12)
119	297			(2, 3, 11)
120	236			(3, 4, 13)
121	311			(2, 3, 11)
122	312			(3, 4, 13)
123				(3, 4, 13)
125	1675			(3, 4, 13)
127	2981			(4, 3, 13)
128				(3, 4, 13)
129				(4, 4, 14)
130	133			(3, 4, 13)
131	277			(3, 4, 13)
134				(3, 4, 13)
135	201			(3, 4, 13)
136	283			(4, 4, 14)
137	234			(1, 3, 10)
138				(2, 4, 12)
139	1677			(2, 4, 12)
147				(6, 6, 20)
149				(3, 4, 13)
151	278			(3, 3, 12)
152	279			(5, 5, 16)
156				(5, 5, 16)
156				(5, 5, 16)
157				(6, 5, 17)
159	275			(2, 3, 11)
161				(6, 5, 17)
169				(3, 7, 24)
170	1674			(4, 4, 14)
171	1670			(5, 5, 16)
172				(5, 5, 16)
189	1664			(6, 5, 17)
190				(4, 4, 14)
195	1673			(6, 4, 16)
196				(6, 5, 17)
206	1666			(5, 5, 16)
207				(3, 4, 14)

Table 8: The orbits of ERs in $\mathcal{R}_{\text{SSA}}^6$ for which we have constructed a holographic graph model. The rows list the ER label s , with color-coding as in Table 4. The columns specify: the corresponding label from [33] for ERs which were previously known (darker), two equivalent graphs (the first with seven boundary vertices, the second with the boundary vertices split so as to avoid cycles containing boundary vertices), and the corresponding graph attributes $\{s,v,e\}$ (specifying the # of splits, # of bulk vertices, and # of edges). To avoid confusion with the values of the edge weights, the parties $0, 1, \dots, 6$ have been relabeled in the various graphs as O, A, \dots, F , respectively.

share the same underlying topology. Furthermore, note that the edge weights have the intriguing property that the sum of the weights of all edges incident on any given vertex is even.

Finally, we remark that some of the ERs with more complicated graphs could potentially have an even simpler graph realization. However, [31] presents a necessary condition for the realizability of an arbitrary entropy vector by a simple tree graph model. We checked this condition for all 220 orbits in $\mathcal{R}_{\text{KC}}^6$ (including the ones that violate SSA), and the only orbits that satisfy this condition are precisely #1 to #44, which are the ones we realized by simple trees. This is perhaps an indication that the condition found in [31] might in fact be sufficient as well.

5.4 Mystery extreme rays

Finally, the six remaining ER orbits, for which we have found neither graph realizations nor any instances of violated HEIs, remain as yet unclassified. It is possible that the complexity of graphs realizing them may be much higher, but it is also possible that they may violate an $N = 6$ HEI not found in [32]. Apart from the absence of both graph realizations and HEI violations, the attributes of these mystery ER orbits do not manifest any obvious differences from either the holographic ERs or the HEI-violating ERs. As we mentioned above, all the orbits in $\mathcal{R}_{\text{SSA}}^6$ which we were able to classify as non-holographic ER orbits violate at least one HEI for $N \leq 5$. These six mystery ER orbits might be an exception, but based on this observation it is tempting to speculate that they are indeed holographic.

6 Discussion

One of the main goals of this work was to present an algorithm for computing the extreme rays of a polyhedral cone when the defining inequalities have a partial order and we are only interested in the ERs corresponding to down-sets. Although we have presented this algorithm in general terms, our primary motivation was to compute the set $\mathcal{R}_{\text{SSA}}^6$, which is the set of ERs of the SAC_6 satisfying SSA, in order to test certain observations and conjectures from previous works (particularly [1, 5, 6]). Indeed, the set $\mathcal{R}_{\text{SSA}}^6$ has turned out to be much richer than the analogous sets for smaller N . Specifically, $\mathcal{R}_{\text{SSA}}^6$ contains 208 orbits of genuine 6-party rays, whereas $\mathcal{R}_{\text{SSA}}^5$ contains only six orbits of genuine 5-party ones. We have already utilized part of the data from this computation to derive new results that have appeared in earlier publications [7, 16]. Here, we highlight some directions for future work, which we organize into two main topics: (1) considerations regarding the algorithm and potential new applications, and (2) comments about open questions specific to the elements of $\mathcal{R}_{\text{SSA}}^6$.

Generalizations and improvements of the algorithm: The algorithm we have presented is tailored to search for KC-ERs, but there are also reasons to compute higher-dimensional KC-faces. For example, as mentioned in the Introduction, the set of all SSA-compatible faces of the SAC_N forms a lattice where the meet operation is simply set intersection. To advance towards solving the quantum marginal independence problem, we can focus on the “building blocks” of this lattice, namely its meet-irreducible

elements. It was shown in [6] that even for $N = 4$, some of these elements are higher-dimensional faces. Furthermore, according to the construction in [7], at least for $N = 4$, these higher-dimensional faces contain projections of SSA-compatible KC-ERs for some $N' > 4$, corresponding to coarse-grainings of the parties. Computing higher-dimensional SSA-compatible faces and ERs for larger N may reveal whether this phenomenon at $N = 4$ is a coincidence, or whether it is indicative of a more general structural property of the SSA-compatible (and perhaps even realizable) faces of the SAC. While ERs are certainly meet-irreducible, higher-dimensional meet-irreducible faces might be harder to find, necessitating a generalization of our algorithm to search for higher-dimensional faces, possibly with further requirements.

Another interesting direction to explore with such a generalization of our algorithm is to search for KC-ERs that have additional intriguing properties. For example, all SSA-compatible KC-ERs for $N \leq 6$ satisfy Ingleton's inequality [36] (which is known to be satisfied by all stabilizer states [15]). This might lead one to speculate that they all lie inside the stabilizer entropy cone, which is unknown for $N \geq 5$. One could then adapt our algorithm to search, at increasing values of N , for SSA-compatible ERs that, for example, violate Ingleton's inequality.

Finally, since these questions are specific to faces of the SAC, it would be worthwhile to explore whether the algorithm could be reformulated using the β -sets technology introduced in [31]. This formulation takes advantage of additional structural properties of SSA-compatible faces and, if incorporated into the algorithm, might help restrict the search space and improve efficiency.

Open questions about the SSA-compatible extreme rays of the 6-party SAC:

The weak form of the conjecture proposed in [1] states that for any given N , all extreme rays of the N -party holographic entropy cone can be obtained from subsystem coarse-grainings of extreme rays in $\mathcal{R}_{\text{Hol}}^{N'}$ for some $N' \geq N$. A stronger form of this conjecture asserts that every extreme ray of the HEC can be realized by a graph model with tree topology (although not necessarily *simple*; that is, not all boundary vertices are required to be labeled by distinct parties).⁵⁰ One of the motivations of this work was to generate data that could be used to corroborate these conjectures.

Out of the 208 orbits of extreme rays (ERs) in $\mathcal{R}_{\text{SSA}}^6$, 52 violate at least one HEI and can therefore be disregarded for this purpose. For the remaining 156 orbits, we were able to construct tree realizations for 148 of them, supporting the strong form of the conjecture. Future attempts to find a counterexample should focus on the remaining eight orbits. Of these, six remain unresolved (see §5.4), as we were unable to determine whether they can be realized by any graph model. It might be worthwhile to explore whether they can be used to propose new HEIs, or if a more focused search could provide a graph realization. The other two orbits (#111 and #207) are definitively holographic, as we did find a graph realization for them, but we were unable to find a tree graph realization. If the strong form of the conjecture is indeed false, perhaps one of these ERs is a counterexample. Proving

⁵⁰ We refer the reader to [1] for the proof that the strong form implies the weak one.

this, however, would require showing that such a tree does not exist for any possible fine-graining to $N' \geq N$ parties, which might necessitate the development of new techniques.

Finally, as previously mentioned, we have not attempted to construct hypergraph models to realize the ERs in §5.2 and §5.4. However, this might be a useful approach to explore whether all these ERs can be realized by stabilizer states and if any of the inclusions in $\mathcal{R}_{\text{HyG}} \subseteq \mathcal{R}_{\text{Sta}} \subseteq \mathcal{R}_{\text{QM}}$ are strict. Of course, obtaining a definitive answer to this question might require more powerful techniques to explore the realizability of the elements of \mathcal{R}_{SSA} beyond stabilizer states, and to determine whether even the inclusion $\mathcal{R}_{\text{QM}} \subseteq \mathcal{R}_{\text{SSA}}$ is strict. This problem, however, is far beyond the scope of this work.

Acknowledgments

We would like to especially thank David Simmons-Duffin for generously providing us supercomputing time in the early iterations of the algorithm. We would also like to thank Sergio Hernández-Cuenca and Sridip Pal for useful discussions.

T.H. is supported by the Heising-Simons Foundation “Observational Signatures of Quantum Gravity” collaboration grant 2021-2817, the U.S. Department of Energy, Office of Science, Office of High Energy Physics, under Award No. DE-SC0011632, and the Walter Burke Institute for Theoretical Physics. V.H. has been supported in part by the U.S. Department of Energy grant DE-SC0009999 and by funds from the University of California. M.R. acknowledges support from UK Research and Innovation (UKRI) under the UK government’s Horizon Europe guarantee (EP/Y00468X/1), and by funds from the University of California during the early stages of this work.

V.H. acknowledges the hospitality of the Kavli Institute for Theoretical Physics (KITP), the Aspen Center for Physics, and the Tsinghua Southeast Asia Center, where part of this work was done. V.H. and M.R. would like to thank the Yukawa Institute for Theoretical Physics for hospitality during the program “Quantum Information, Quantum Matter and Quantum Gravity” during the early stages of this work.

All data is available within the paper and as an ancillary file in the arXiv. The code used to generate and analyze this data is a combination of a Wolfram Mathematica implementation of the algorithm outlined in this work, and the freely available software Normaliz [18].

References

- [1] S. Hernández-Cuenca, V. E. Hubeny, and M. Rota, “The holographic entropy cone from marginal independence,” *JHEP* **09** (2022) 190, [arXiv:2204.00075 \[hep-th\]](#).
- [2] J. M. Maldacena, “The Large N limit of superconformal field theories and supergravity,” *Adv. Theor. Math. Phys.* **2** (1998) 231–252, [arXiv:hep-th/9711200](#).
- [3] S. S. Gubser, I. R. Klebanov, and A. M. Polyakov, “Gauge theory correlators from noncritical string theory,” *Phys. Lett. B* **428** (1998) 105–114, [arXiv:hep-th/9802109](#).
- [4] E. Witten, “Anti-de Sitter space and holography,” *Adv. Theor. Math. Phys.* **2** (1998) 253–291, [arXiv:hep-th/9802150](#).

- [5] S. Hernández-Cuenca, V. E. Hubeny, M. Rangamani, and M. Rota, “The quantum marginal independence problem,” [arXiv:1912.01041 \[quant-ph\]](#).
- [6] T. He, V. E. Hubeny, and M. Rota, “On the relation between the subadditivity cone and the quantum entropy cone,” *JHEP* **08** (2023) 018, [arXiv:2211.11858 \[hep-th\]](#).
- [7] T. He, V. E. Hubeny, and M. Rota, “Inner bounding the quantum entropy cone with subadditivity and subsystem coarse grainings,” *Phys. Rev. A* **109** no. 5, (2024) 052407, [arXiv:2312.04074 \[quant-ph\]](#).
- [8] N. Bao, S. Nezami, H. Ooguri, B. Stoica, J. Sully, and M. Walter, “The Holographic Entropy Cone,” *JHEP* **09** (2015) 130, [arXiv:1505.07839 \[hep-th\]](#).
- [9] S. Ryu and T. Takayanagi, “Holographic derivation of entanglement entropy from AdS/CFT,” *Phys. Rev. Lett.* **96** (2006) 181602, [arXiv:hep-th/0603001 \[hep-th\]](#).
- [10] V. E. Hubeny, M. Rangamani, and T. Takayanagi, “A Covariant holographic entanglement entropy proposal,” *JHEP* **07** (2007) 062, [arXiv:0705.0016 \[hep-th\]](#).
- [11] N. Pippenger, “The inequalities of quantum information theory,” *IEEE Transactions on Information Theory* **49** no. 4, (2003) 773–789.
- [12] N. Linden and A. Winter, “A new inequality for the von neumann entropy,” *Communications in Mathematical Physics* **259** no. 1, (2005) 129–138. <https://doi.org/10.1007/s00220-005-1361-2>.
- [13] J. Cadney, N. Linden, and A. Winter, “Infinitely many constrained inequalities for the von neumann entropy,” *IEEE Transactions on Information Theory* **58** no. 6, (2012) 3657–3663.
- [14] M. Christandl, B. Durhuus, and L. H. Wolff, “Tip of the quantum entropy cone,” *Physical Review Letters* **131** no. 24, (Dec., 2023) . <http://dx.doi.org/10.1103/PhysRevLett.131.240201>.
- [15] N. Linden, F. Matúš, M. B. Ruskai, and A. Winter, “The Quantum Entropy Cone of Stabiliser States,” *Leibniz Int. Proc. Inf.* **22** (2013) 270–284, [arXiv:1302.5453 \[quant-ph\]](#).
- [16] T. He, V. E. Hubeny, and M. Rota, “Gap between holographic and quantum mechanical extreme rays of the subadditivity cone,” *Phys. Rev. D* **109** no. 4, (2024) L041901, [arXiv:2307.10137 \[hep-th\]](#).
- [17] V. E. Hubeny, M. Rangamani, and M. Rota, “The holographic entropy arrangement,” *Fortsch. Phys.* **67** no. 4, (2019) 1900011, [arXiv:1812.08133 \[hep-th\]](#).
- [18] W. Bruns, B. Ichim, C. Söger, and U. von der Ohe, “Normaliz. Algorithms for rational cones and affine monoids.” Available at <https://www.normaliz.uni-osnabrueck.de>.
- [19] N. Bao, N. Cheng, S. Hernández-Cuenca, and V. P. Su, “The Quantum Entropy Cone of Hypergraphs,” *SciPost Phys.* **9** no. 5, (2020) 5, [arXiv:2002.05317 \[quant-ph\]](#).
- [20] M. Walter and F. Witteveen, “Hypergraph min-cuts from quantum entropies,” *J. Math. Phys.* **62** no. 9, (2021) 092203, [arXiv:2002.12397 \[quant-ph\]](#).
- [21] E. H. Lieb and M. B. Ruskai, “Proof of the strong subadditivity of quantum-mechanical entropy,” *J. Math. Phys.* **14** (1973) 1938–1941.
- [22] M. A. Nielsen and I. L. Chuang, *Quantum Computation and Quantum Information: 10th Anniversary Edition*. Cambridge University Press, 2010.
- [23] S. Hernández Cuenca, “Holographic entropy cone for five regions,” *Phys. Rev. D* **100** no. 2, (2019) 026004, [arXiv:1903.09148 \[hep-th\]](#).

- [24] V. Hubeny and M. Rota, “Observations on the SSA-compatible extreme rays of the subadditivity cone for $N = 6$,”. In preparation.
- [25] G. Birkhoff, *Lattice Theory*. American Mathematical Society, Providence, 3rd ed., 1967.
- [26] T. H. Matheiss and D. S. Rubin, “A survey and comparison of methods for finding all vertices of convex polyhedral sets,” *Mathematics of Operations Research* **5** no. 2, (1980) 167–185. <https://doi.org/10.1287/moor.5.2.167>.
- [27] G. M. Ziegler, *Lectures on polytopes*. Springer-Verlag, New York, 1995. <https://doi.org/10.1007/978-1-4613-8431-1>.
- [28] K. Fukuda, *Lectures on Polyhedral Computation*. ETH Zurich, 2015. <https://people.inf.ethz.ch/fukudak/lect/pcllect/notes2015/PolyComp2015.pdf>.
- [29] D. Bremner, M. D. Sikiric, and A. Schuermann, “Polyhedral representation conversion up to symmetries,” *CRM Proceedings & Lecture Notes* **48** (2009) 45–71, [arXiv:math/0702239](https://arxiv.org/abs/math/0702239) [math.MG]. <https://arxiv.org/abs/math/0702239>.
- [30] A. Björner, M. Las Vergnas, B. Sturmfels, N. White, and G. M. Ziegler, *Oriented matroids*, vol. 46 of *Encyclopedia of Mathematics and its Applications*. Cambridge University Press, Cambridge, 1993.
- [31] V. Hubeny and M. Rota, “Correlation hypergraph: a new representation of a quantum marginal independence pattern,”. In preparation.
- [32] S. Hernández-Cuenca, V. E. Hubeny, and H. F. Jia, “Holographic entropy inequalities and multipartite entanglement,” *JHEP* **08** (2024) 238, [arXiv:2309.06296](https://arxiv.org/abs/2309.06296) [hep-th].
- [33] S. Hernández-Cuenca, “Holographic Entropy Cone Database,” *GitHub Repository* (2024) .
- [34] P. Hayden, M. Headrick, and A. Maloney, “Holographic Mutual Information is Monogamous,” *Phys. Rev.* **D87** no. 4, (2013) 046003, [arXiv:1107.2940](https://arxiv.org/abs/1107.2940) [hep-th].
- [35] N. Bao, N. Cheng, S. Hernández-Cuenca, and V. P. Su, “A Gap Between the Hypergraph and Stabilizer Entropy Cones,” [arXiv:2006.16292](https://arxiv.org/abs/2006.16292) [quant-ph].
- [36] A. W. Ingleton, “Representation of matroids.” *Combinat. Math. Appl., Proc. Conf. math. Inst., Oxford 1969, 149-167 (1971).*, 1971.